

Journal Pre-proofs

On disclosing the role of mesoporous alumina in the ozonation of sulfamethoxazole: adsorption vs. catalysis

Carla di Luca, Natalia Inchaurredo, Mireia Marcé, Rodrigo Parra, Santiago Esplugas, Patricia Haure

PII: S1385-8947(21)00178-9
DOI: <https://doi.org/10.1016/j.cej.2021.128579>
Reference: CEJ 128579

To appear in: *Chemical Engineering Journal*

Received Date: 3 September 2020
Revised Date: 9 January 2021
Accepted Date: 14 January 2021

Please cite this article as: C. di Luca, N. Inchaurredo, M. Marcé, R. Parra, S. Esplugas, P. Haure, On disclosing the role of mesoporous alumina in the ozonation of sulfamethoxazole: adsorption vs. catalysis, *Chemical Engineering Journal* (2021), doi: <https://doi.org/10.1016/j.cej.2021.128579>

This is a PDF file of an article that has undergone enhancements after acceptance, such as the addition of a cover page and metadata, and formatting for readability, but it is not yet the definitive version of record. This version will undergo additional copyediting, typesetting and review before it is published in its final form, but we are providing this version to give early visibility of the article. Please note that, during the production process, errors may be discovered which could affect the content, and all legal disclaimers that apply to the journal pertain.

© 2021 Elsevier B.V. All rights reserved.



sulfamethoxazole: adsorption vs. catalysis

Carla di Luca^{a,*}, Natalia Inchaurredo^a, Mireia Marcé^b, Rodrigo Parra^c, Santiago Esplugas^b and Patricia Haure^a

^a Div. Catalizadores y Superficies. Instituto de Investigaciones en Ciencia y Tecnología de Materiales (INTEMA-CONICET). Departamento de Ingeniería Química-Facultad de Ingeniería, Universidad Nacional de Mar del Plata. Av. J. B. Justo 4302 (B7608FDQ), Mar del Plata, Argentina.

^b Department of Chemical Engineering and Analytical Chemistry, Faculty of Chemistry, Universitat de Barcelona, C/Martí i Franqués 1, 08028 Barcelona, Spain.

^c Div. Cerámicos. Instituto de Investigaciones en Ciencia y Tecnología de Materiales (INTEMA), CONICET-UNMdP, Av. Colón 10850 (B7606BWV), Mar del Plata, Argentina.

*Correspondence to: cardiluca@fi.mdp.edu.ar

Abstract

Ordered mesoporous alumina (MA) and Fe-doped MA were synthesized by evaporation-induced self-assembly and tested for the ozonation of sulfamethoxazole (SMX). The synthesis methodology produced MA whose surface and structural properties exceeded those of commercial types displaying a BET surface area of 263 m²/g, a pore volume of 0.8 cm³/g and aligned cylindrical pores of c.a. 10 nm. The ozonation of SMX (20 mg/L) was performed in a semibatch stirred tank reactor at: T = 22 °C, [O₃]_{gas} = 10 mg/L, Q_{gas} = 42 L/h NTP, [solid] ≈ 1 g/L, t = 120 min. Single ozonation achieved fast and complete SMX removal and mineralized up to 35% of the organics at neutral pH. The addition of MA or Fe-doped MA did not affect the removal rate of SMX, but did achieve a remarkable TOC removal up to 86% at acid pH. However, under the selected operating conditions, ferric species did not improve the removal of organic matter. Then, the adsorption and catalytic contribution of MA was evaluated in specifically-designed experiments. While SMX adsorption was low, its oxidation intermediates did adsorb onto MA surface. Despite the high ability of the

materials to decompose ozone, the results revealed that the by-products adsorption is the prevailing process for the TOC removal. After four successive reuses, MA reduced its adsorption performance due to chemisorption of carboxylates. Nevertheless, the worn material was regenerated by direct ozonation in gas phase. In addition, primary transformation products were identified by LC-ESI-TOF-MS and the scavenging effect of the water matrix was assessed using bottled water and a real secondary wastewater.

Key-words: OZONATION, ORDERED MESOPOROUS ALUMINA, EMERGING POLLUTANTS, SULFAMETHOXAZOLE, ADSORPTION.

1. Introduction

Water pollution by pharmaceuticals (PhACs) represents an emerging environmental problem. Although these micropollutants can be found in very low concentrations, concern is related to their potential negative consequences on aquatic ecosystems and public health systems [1,2]. While conventional treatment technologies were not designed to remove these types of compounds, adsorption processes and/or oxidation technologies, such as Advanced Oxidation Processes (AOPs) and ozonation, can provide interesting treatment alternatives for the removal of PhACs in aqueous solutions [3–5].

Among PhACs, sulfamethoxazole (SMX) is a sulfonamide antibiotic widely prescribed to treat bacterial infections in humans and animals, and frequently detected in the aquatic environment. The occurrence of SMX in the aquatic environment has been shown to induce genetic mutations and chronic effects even at trace concentrations [3,6]. Hence, it is essential to control the antibiotic level in aquatic environments and to develop treatment facilities for the removal of these compounds, especially when reclaimed wastewater is required [2].

Ozone is a powerful oxidizing agent, which effectively breaks up the chemical bonds of complex molecules, making it an efficient method to remove PhACs from wastewater. However, single ozonation only achieves limited mineralization of organic compounds. Its inefficacy is mainly due to its electrophilic nature and the selectivity of reactions [2,7]. So as to intensify the ozonation process and promote less selective removal pathways, ozone has been combined with solid materials such as catalysts or adsorbents [3,8,9].

Heterogeneous catalytic ozonation consists in the incorporation of solid materials with a view to promoting the transformation of ozone into more powerful and non-selective active species such as •OH radicals or

other reactive oxygen species. In addition, it seeks to facilitate chemisorption of organic molecules and/or ozone on the catalyst's surface sites and their further interaction [9,10]. Adsorption instead, allows the separation of organic molecules by chemisorption at the surface sites of the material, meaning low initial investment, simpler reactor design, operational simplicity and an unselective nature [11]. In both cases, the effectiveness of the treatment technology depends to a great extent on the surface properties of the material, the nature of the organic molecules, as well as the pH of the effluent, which influences surface properties and ozone decomposition reactions in aqueous solutions [11,12].

Alumina is a typical adsorbent and one of the most widely used catalytic support due to its good mechanical, electric and chemical properties and relatively low cost. It is an amphoteric material, with a pore size distribution easily changeable and presents different crystalline structures. The usefulness of transition aluminas can be traced to a favorable combination of textural properties (i.e. surface area, pore volume, and pore size distribution), acid-base characteristics and on the degree of hydration and hydroxylation of the surface [13]. The extension of these features is strongly dependent on the preparation method and the used pre-treatments conditions. During thermal treatment, the removal of surface OH groups (Brønsted acid sites) creates a coordinatively unsaturated surface of Al cations at the octahedral and tetrahedral sites. The partly uncoordinated metal cations and oxide anions that lie at the alumina surface can act as Lewis acids and bases, respectively [13,14]. As a result, the true peculiar sites of aluminas are very likely anion–cation couples which have very high activity and work synergistically [15].

Organized mesoporous aluminas (MA) are a new family of porous materials, the properties of which significantly extend the properties of conventional aluminas, due to the possibility of tailoring surface areas, void volumes and pore sizes; which are highly desirable features for heterogeneous catalysis and adsorption processes. Moreover, these materials allow the incorporation of active species through different methodologies, obtaining functional materials with greater reactivity and selectivity [16]. Among different preparation methodologies, sol-gel is one of the most preferred methods for the synthesis of mesoporous metal oxides since it provides a low-temperature synthesis route with excellent control over mixing [13]. Based on the sol-gel methodology, a remarkable way of achieving the growth of ordered MA structures is the solvent Evaporation-Induced Self-Assembly (EISA). The EISA methodology ensures organized mesoporous aluminas with high purity, fine-tuned structural properties (high surface area and narrow pore size distribution) and high surface acidity. This one-pot strategy involves introducing molecular metal

precursors into a solution of non-ionic surfactants (as structure-directing agent), with strict adjustment of the reactants' molar ratios [17,18]. Furthermore, one of the main drawbacks of liquid-phase oxidation is deactivation by leaching of active species [19]. In this sense, this methodology allows direct incorporation of active components (such as transition metals) during the synthesis of the porous matrix, which improves both the homogeneous distribution of active centers and catalytic stability, preventing the leaching of active components while improving its anchorage to the porous matrix [20].

Despite years of research in catalytic ozonation, there is a poor understanding of the mechanisms involved in the oxidation of organic molecules, so the process has not been widely applied on a larger scale. Until now, the mechanisms of catalytic ozonation with alumina have raised several controversies. For some researchers, alumina is an active catalyst while for others just acts as an adsorbent [21]. Hereof, the literature reveals that the adsorption contribution has not always been assessed properly, and that sometimes only the adsorption of the parent compound is evaluated, while only few works consider the adsorption of reaction intermediates [22–27]. Likewise, false catalytic activity of commercial aluminum oxides has been registered due to the presence of alkaline impurities which increase the pH of the water [28]. Also, several studies report single ozonation and catalytic ozonation without accurate pH control, which can lead to observation of an “apparent” catalytic effect due to ozone decomposition [21]. Another important aspect is catalyst stability, when leaching occurs, the traces of dissolved cations might catalyze the mineralization of organic matter [29,30]. Hence, several operating parameters must be taken into account to avoid experimental errors: i) characterization of the surface properties of the solids; ii) contribution of the support before being doped with metallic species; iii) pH measurements along the reaction time; iv) adsorption contribution of the main pollutant as well as its reaction by-products; v) catalyst stability and contribution of leached metals even at trace levels; vi) formation of $\bullet\text{OH}$ radicals and vii) reusability of the solid material.

Table 1 and Table 2 compile literature results employing alumina for the ozonation of organic matter and different solid materials for the abatement of SMX, respectively. As can be seen, the systems have been investigated over a wide range of operating conditions (pH, ozone dosage, mass ratio between solid and organic matter load, etc.) and that is why the existing proposals are difficult to compare. In this study, the results obtained are discussed and compared with the most relevant proposals reported in the bibliography. The research methodology applied seeks to avoid the typical experimental errors commented above. To

accomplish this, specific ozonation experiments were performed to discriminate the catalytic effect from the adsorption contribution (parent compound and reaction intermediates).

In a previous work, it was demonstrated the efficacy of ordered mesoporous alumina (MA) in the adsorption of dominant arsenic species present in water [31]. In the present study, the objectives are: i) to develop a fine-tuned material based on mesoporous alumina to improve the removal of organic matter with ozone; ii) to study the performance of the material in the ozonation of SMX; iii) to assess the influence of Fe incorporation during the synthesis of MA as well as its ozonation performance; and iv) to provide further understanding of the mechanisms of SMX ozonation in the presence of ordered mesoporous alumina. Up to the present, most of the studies on catalytic ozonation with alumina were carried out by using commercial materials. To avoid the presence of impurities, ordered mesoporous alumina of high purity was synthesized by means of a novel methodology, Evaporation-Induced Self-Assembly, and tested in the ozonation of sulfamethoxazole. Moreover, since Fe-doped catalysts have been widely used for the removal of emerging pollutants due to their affordability and high levels of activity [10], the addition of Fe during the synthesis of MA was under study.

Table 1. Literature reports on alumina and Fe-doped alumina for the ozonation of organic pollutants.

Pollutant	Solid material	Operating conditions	Removal results	Ref.
Humic substances TOC ₀ = 2.5-2.6 mg/L	Al ₂ O ₃	cat. 130 g/L, V _{liq} = 46 mL, room T, pH 7.2, O ₃ 2.5 mg/mg _{TOC} , t _{test} = 10 min, Slurry Batch reactor	Ads. X _{TOC} = 44 % O ₃ X _{TOC} = 13.8 % O ₃ + cat. X _{TOC} = 47.2 %	[32]
Salicylic acid TOC ₀ = 3 mg/L	Al ₂ O ₃	cat. 130 g/L, V _{liq} = 46 mL, room T, pH 7.2, O ₃ 2.5 mg/mg _{TOC} , t _{test} = 10 min, Slurry Batch reactor	Ads. X _{TOC} = 51.7 % O ₃ X _{TOC} = 12.7 % O ₃ + cat. X _{TOC} = 52.3 %	[32]
Peptide TOC ₀ = 2.5-2.6 mg/L	Al ₂ O ₃	cat. 130 g/L, V _{liq} = 46 mL, room T, pH 7.2, O ₃ 2.5 mg/mg _{TOC} , t _{test} = 10 min, Slurry Batch reactor	Ads. X _{TOC} = 0 % O ₃ X _{TOC} = 46 % O ₃ + cat. X _{TOC} = 15.4 %	[32]
Oxalic acid 0.008 mol/L	γ-Al ₂ O ₃	cat. 1.25 g/L, V _{liq} = 800 mL, 20 °C, pH 2.5, Q _{gas} = 24 L/h, [O ₃] _{gas} = 30 mg/L, t _{test} = 3 h, SemiBatch reactor	O ₃ X _{oxalic} = 1-2 % O ₃ + cat. X _{oxalic} = 7 %	[33]
Oxalic acid 0.008 mol/L	γ-Al ₂ O ₃ -Fe ₂ O ₃	cat. 1.25 g/L, V _{liq} = 800 mL, 20 °C, pH 2.5, Q _{gas} = 24 L/h, [O ₃] _{gas} = 30 mg/L, t _{test} = 3 h, SemiBatch reactor	Ads. X _{oxalic} = 7 % O ₃ X _{oxalic} = 1-2 % O ₃ + cat. X _{oxalic} = 28 %	[33]
Bisphenol A 10 mg/L	γ-Al ₂ O ₃	cat. 1 g/L, 23 °C, pH ₀ 5, [O ₃] _{liq} = 4.5 mg/L, t _{test} = 1 h, Slurry Batch reactor	Ads. X _{TOC} = 87 % O ₃ X _{TOC} = 35 % O ₃ + cat. X _{TOC} = 90 %	[26]
2,4 dimethylphenol 50 mg/L	γ-Al ₂ O ₃	cat. 5 g/L, V _{liq} = 1.5 L, 25 °C, pH ₀ 4.5, Q _{gas} = 40 L/h, [O ₃] _{gas} = 2 g/Nm ³ , t _{test} = 300 min, Slurry SemiBatch reactor	O ₃ X _{TOC} = 14 % O ₃ + cat. X _{TOC} = 57 % Carboxylic acid adsorbed are difficult to accurately estimate	[27]

Tap water enriched with NOM DOC 28.7 mg/L	Al ₂ O ₃	cat. 30 g, V _{liq} = 0.4 L, 20 °C, pH 8, Q _{gas} = 19.5 mL/min, [O ₃] _{gas} = 0.4 mg/L min, t _{test} = 3 h, Fixed bed reactor semibatch	17 cycles O ₃ X _{TOC} = 31 % O ₃ + cat. X _{TOC} = 63 % Adsorption is the dominant process during the first cycles	[34]
Dimethyl phthalate (DMP) TOC ₀ = 4.03 mg/L	Al ₂ O ₃	cat. 10 g/L, 15 °C, pH ₀ 6.6, Q _{gas} = 0.4 L/min, [O ₃] _{dose} = 116 mg/h, t _{test} = 2 h, Slurry SemiBatch reactor	Ads. X _{DMP} = 5 % O ₃ X _{TOC} = 24 % O ₃ + cat. X _{TOC} = 56 % Byproducts adsorption could not be neglected	[35]
Ibuprofen 15 mg/L	γ-Al ₂ O ₃	cat. 5 g, V _{liq} = 0.49 L, 20 °C, pH 7.2, Q _{gas} = 0.5 mL/min, [O ₃] _{dose} = 0.5 mg/min, t _{test} = 30 min, Fixed bed SemiBatch reactor	Ads. X _{ibuprofen} = 13 % O ₃ X _{ibuprofen} = 40 % O ₃ + cat. X _{ibuprofen} = 83 %	[25]
Acetic acid 15 mg/L	γ-Al ₂ O ₃	cat. 5 g, V _{liq} = 0.49 L, 20 °C, pH 7.2, Q _{gas} = 0.5 mL/min, [O ₃] _{dose} = 0.5 mg/min, t _{test} = 30 min, Fixed bed SemiBatch reactor	Ads. X _{acetic} = 7 % O ₃ X _{acetic} = 6 % O ₃ + cat. X _{acetic} = 19 %	[25]
Cumene 19.1 mg/L	γ-Al ₂ O ₃	cat. 5 g, V _{liq} = 0.49 L, 20 °C, pH 7.2, Q _{gas} = 0.1 mL/min, [O ₃] _{dose} = 0.1 mg/min, t _{test} = 30 min, Fixed bed SemiBatch reactor	Ads. X _{cumene} = 5 %, O ₃ X _{cumene} = 60 %, O ₃ + cat. X _{cumene} = 58 %	[25]
1,2-dichlorobenzene 3.5 mg/L	γ-Al ₂ O ₃	cat. 5 g, V _{liq} = 0.49 L, 20 °C, pH 6.2, Q _{gas} = 0.1 mL/min, [O ₃] _{dose} = 0.1 mg/min, t _{test} = 30 min, Fixed bed SemiBatch reactor	Ads. X _{dichlorobenzene} = 7 % O ₃ X _{dichlorobenzene} = 61 % O ₃ + cat. X _{dichlorobenzene} = 45 %	[25]
2-isopropyl-3-methoxypyrazine (IPMP) 38 μg/L	γ-Al ₂ O ₃	cat. 500 mg/L, pH 7.05, [O ₃] _{liq} = 0.5 mg/L, t _{test} = 10 min, Slurry Batch reactor	Ads. X _{IPMP} = 5 % O ₃ X _{IPMP} = 55 % O ₃ + cat. X _{IPMP} = 90 %	[36]
m-dinitrobenzene 1 mmol/L	Al ₂ O ₃	cat. 1 g/L, V _{liq} = 0.7 L, 20 °C, pH ₀ 3, Q _{gas} = 1 L/min, [O ₃] _{gas} = 12 mg/L, t _{test} = 2 h, Bubble Column SemiBatch reactor	O ₃ X _{COD} = 68 % O ₃ + cat. X _{COD} = 92 %	[37]
Paracetamol 35 μmol/L	Al ₂ O ₃	cat. 5 mg/L, V _{liq} = 0.7 L, pH 3, [O ₃] _{dose} = 3 mg/min, t _{test} = 1 h, Slurry SemiBatch reactor	O ₃ X _{TOC} = 4 %, O ₃ + cat. X _{TOC} = 10.13 % probably due to adsorption	[38]
Paracetamol 35 μmol/L	γ-Al ₂ O ₃	cat. 5 mg/L, pH 7, [O ₃] _{dose} = 3 mg/min, t _{test} = 1 h, SemiBatch reactor	O ₃ X _{TOC} = 18 % O ₃ + cat. X _{TOC} = 17.2 %	[38]
Oxalic acid TOC ₀ = 60 mg/L	γ-Al ₂ O ₃	cat. 50 g/L, V _{liq} = 40 mL, pH 3.3, [O ₃] _{gas} = 50 g/Nm ³ , t _{test} = 30 min, Batch reactor	Ads. X _{TOC} = 71.9 % O ₃ X _{TOC} = 26.5 % O ₃ + cat. X _{TOC} = 73.6 %	[23]
Oxalic acid TOC ₀ = 60 mg/L	γ-Al ₂ O ₃	cat. 50 g/L, V _{liq} = 40 mL, pH 5 (buffer orthophosphate), [O ₃] _{gas} = 50 g/Nm ³ , t _{test} = 30 min, Batch reactor	Ads. X _{TOC} = 8.8 % O ₃ X _{TOC} = 0.2 % O ₃ + cat. X _{TOC} = 19 %	[23]
Acetic acid TOC ₀ = 60 mg/L	γ-Al ₂ O ₃	cat. 50 g/L, V _{liq} = 40 mL, pH 3.3, [O ₃] _{gas} = 50 g/Nm ³ , t _{test} = 30 min, Batch reactor	Ads. X _{TOC} = 5.1 % O ₃ X _{TOC} = 4.2 % O ₃ + cat. X _{TOC} = 7.7 %	[23]
Acetic acid TOC ₀ = 60 mg/L	γ-Al ₂ O ₃	cat. 50 g/L, V _{liq} = 40 mL, pH 5 (buffer orthophosphate), [O ₃] _{gas} = 50 g/Nm ³ , t _{test} = 30 min, Batch reactor	Ads. X _{TOC} = 0 % O ₃ X _{TOC} = 2.2 % O ₃ + cat. X _{TOC} = 0 %	[23]
Salicylic acid TOC ₀ = 60 mg/L	γ-Al ₂ O ₃	cat. 50 g/L, V _{liq} = 40 mL, pH 3.3, [O ₃] _{gas} = 50 g/Nm ³ , t _{test} = 30 min, Batch reactor	Ads. X _{TOC} = 60.8 % O ₃ X _{TOC} = 38.6 % O ₃ + cat. X _{TOC} = 89.9 %	[23]
Salicylic acid TOC ₀ = 60 mg/L	γ-Al ₂ O ₃	cat. 50 g/L, V _{liq} = 40 mL, pH 5 (buffer orthophosphate), [O ₃] _{gas} = 50 g/Nm ³ , t _{test} = 30 min, Batch reactor	Ads. X _{TOC} = 41.4 % O ₃ X _{TOC} = 44.9 % O ₃ + cat. X _{TOC} = 83.5 %	[23]

Succinic acid TOC ₀ = 60 mg/L	γ -Al ₂ O ₃	cat. 50 g/L, V _{liq} = 40 mL, pH 3.3, [O ₃] _{gas} = 50 g/Nm ³ , t _{test} = 30 min, Batch reactor	Ads. X _{TOC} = 24.2 % O ₃ X _{TOC} = 5.8 % O ₃ + cat. X _{TOC} = 87.5 %	[23]
Succinic acid TOC ₀ = 60 mg/L	γ -Al ₂ O ₃	cat. 50 g/L, V _{liq} = 40 mL, pH 5 (buffer orthophosphate), [O ₃] _{gas} = 50 g/Nm ³ , t _{test} = 30 min, Batch reactor	Ads. X _{TOC} = 0.4 % O ₃ X _{TOC} = 0 % O ₃ + cat. X _{TOC} = 69.2 %	[23]
Succinic acid TOC ₀ = 60 mg/L	χ - and η -Al ₂ O ₃	cat. 50 g/L, V _{liq} = 40 mL, pH 5 (buffer orthophosphate), [O ₃] _{gas} = 50 g/Nm ³ , t _{test} = 30 min, Batch reactor	Ads. X _{TOC} = 18.8 % O ₃ + cat. X _{TOC} = 35 %	[23]
Succinic acid TOC ₀ = 60 mg/L	χ - and η -Al ₂ O ₃	cat. 20 g/L, V _{liq} = 5.2 L, pH 7, Q _{gas} = 100 L/h, [O ₃] _{gas} = 50 g/Nm ³ , t _{test} = 1 h, Slurry SemiBatch reactor	O ₃ X _{TOC} = 23 % O ₃ + cat. X _{TOC} = 90 %	[23]
Diclofenac 30 mg/L	γ -Al ₂ O ₃	cat. 5 g, V _{liq} = 250 mL, pH 7 or 5, Q _{gas} = 25 L/h, [O ₃] _{gas} = 20 mg/L, t _{test} = 2 h, Batch reactor	O ₃ X _{TOC} = 40 %, pH 7: O ₃ + cat. X _{TOC} = 65 % pH 5: O ₃ + cat. X _{TOC} = 40 % Adsorption of carboxylates was confirmed	[39]
2-methylisoborneol (MIB) 22 μ g/L	γ -Al ₂ O ₃	cat. 500 mg/L, V _{liq} = 1 L, 20°C, pH 6.6, [O ₃] _{liq} = 0.5 mg/L, t _{test} = 20 min, Batch reactor	Ads. X _{MIB} = 2.5 % O ₃ X _{MIB} = 40 % O ₃ + cat. X _{MIB} = 87 %	[40]
4-chloro-7-nitrobenzo-2-oxa-1,3-dizole (NBD-Cl) 20 mg/L	γ -Al ₂ O ₃	cat. 2 g, V _{liq} = 0.49 L, 25°C, pH 8.8, [O ₃] _{dose} = 0.6 mg/min, t _{test} = 30 min, SemiBatch reactor	Ads. X _{NBD-Cl} = 4-5 % O ₃ X _{NBD-Cl} = 40 % O ₃ + cat. X _{NBD-Cl} = 72 %	[41]
2-chlorophenol (CP) 100 mg/L	γ -Al ₂ O ₃	cat. 2 g/L, pH 7, [O ₃] _{dose} = 18 mg/min, t _{test} = 90 min, SemiBatch reactor	Ads. X _{CP} = 1.1-2.2 % O ₃ X _{TOC} = 21 % O ₃ + cat. X _{TOC} = 43 %	[42]
2, 4, 6-trichloroanisole (TCA) 25 μ g/L	γ -Al ₂ O ₃	cat. 200 mg/L, V _{liq} = 1 L, 20 °C, pH 5.8, [O ₃] _{liq} = 0.5 mg/L, t _{test} = 10 min, Batch reactor	Ads. X _{TCA} = 10 % O ₃ X _{TCA} = 40 % O ₃ + cat. X _{TCA} = 62 %	[43]
Ibuprofen 10 mg/L	γ -Al ₂ O ₃	cat. 1.5 g/L, V _{liq} = 1 L, 20°C, pH ₀ 7, Q _{gas} = 12 L/h, [O ₃] _{gas} = 30 mg/L, t _{test} = 40 min, SemiBatch reactor	O ₃ X _{TOC} = 20 % O ₃ + cat. X _{TOC} = 54 %	[44]
Ibuprofen (IBU) 10 mg/L	β -FeOOH/ γ -Al ₂ O ₃	cat. 1.5 g/L, V _{liq} = 1 L, 20°C, pH ₀ 7, Q _{gas} = 12 L/h, [O ₃] _{gas} = 30 mg/L, t _{test} = 40 min, SemiBatch reactor	Ads. X _{IBU} < 5 % O ₃ X _{TOC} = 20 % O ₃ + cat. X _{TOC} = 90 %	[44]
m-cresol 9.52 mol/L	γ -Al ₂ O ₃	cat. 10 g/L, V _{liq} = 25 mL, 20 °C, Q _{gas} = 0.5 L/min, [O ₃] _{gas} = 0.123 mg/L, t _{test} = 24 h, SemiBatch reactor	O ₃ X _{m-cresol} = 22.5 % O ₃ + cat. X _{m-cresol} = 47 %	[45]
Sulfamethoxazole TOC ₀ = 15 mg/L	Al ₂ O ₃	20°C, pH 7, Q _{gas} = 24 L/h, [O ₃] _{gas} = 20 mg/L, t _{test} = 2 h, Slurry SemiBatch reactor	O ₃ X _{TOC} = 28 % O ₃ + cat. X _{TOC} = 39 %	[22]
Textile wastewater COD ₀ = 180 mg/L	Al ₂ O ₃	cat. 300 g, pH 4, Q _{liq} = 250 L/h, Q _{gas} = 340 L/h, expanded bed height = 17 cm, [O ₃] _{gas} = 0.9 mmol/L, Continuous fluidized bed reactor	O ₃ X _{COD} = 16.49 % O ₃ + cat. X _{COD} = 25.83 %	[46]
Petroleum refinery wastewater COD ₀ = 101.3 mg/L	γ -Al ₂ O ₃	cat. 0,5 g, V _{liq} = 100 mL, 30°C, pH 8.15, O ₃ 5 mg/min, t _{test} = 40 min, Slurry SemiBatch reactor	Ads. X _{COD} = 8.5 % O ₃ X _{COD} = 34.3 % O ₃ + cat. X _{COD} = 45.9 %	[47]
Fluoxetene 30 mg/L	γ -Al ₂ O ₃	cat. 1 g/L, V _{liq} = 200 mL, 25°C, pH 7, [O ₃] _{gas} = 30 mg/L, t _{test} = 17 min, Slurry SemiBatch reactor	O ₃ X _{fluox} = 80 % O ₃ + cat. X _{fluox} = 86 %	[48]
Naphtenic acids 100 mg/L	γ -Al ₂ O ₃	cat. 1 g/L, 25°C, pH 8.5, Q _{gas} = 1 L/min, t _{test} = 50 min, Slurry Batch reactor	Ads. X _{naph} = 8 % O ₃ X _{naph} = 85 % O ₃ + cat. X _{naph} = 88 %	[49]

Humic acids 50 mg/L	α -Al ₂ O ₃	cat. 0.5 g/L, 25 °C, pH 5.5, O ₃ 0.063 m ³ /h, t _{test} = 1 h, Slurry Batch reactor	Ads. X _{humic} = 90 % O ₃ X _{humic} = 81 % O ₃ + cat. X _{humic} = 100 %	[50]
Landfill leachate COD ₀ = 1317.5 mg/L	γ -Al ₂ O ₃	cat. 50 g/L, V _{liq} = 300 mL, 30°C, pH ₀ 7.3, O ₃ 22 mg/min, t _{test} = 30 min, Slurry SemiBatch reactor	Ads. X _{COD} = 27 % O ₃ X _{COD} = 48 % O ₃ + cat. X _{COD} = 70 %	[51]

Table 2. Literature reports on different solids in the ozonation of SMX.

SMX Concentration	Solid material	Operating conditions	Removal results	Ref.
TOC ₀ = 15 mg/L	Al ₂ O ₃	20 °C, pH 7, Q _{gas} = 24 L/h, [O ₃] _{gas} = 25 mg/L, t _{test} = 2 h, Slurry SemiBatch reactor	Ads. X _{SMX} = 7 % O ₃ X _{TOC} = 28 % O ₃ + cat. X _{TOC} = 39 %	[22]
TOC ₀ = 15 mg/L	LaTi _{0.15} Cu _{0.05} O ₃	20 °C, pH 7, Q _{gas} = 24 L/h, [O ₃] _{gas} = 25 mg/L, t _{test} = 2 h, Slurry SemiBatch reactor	Ads. X _{SMX} = 1 % O ₃ X _{TOC} = 28 % O ₃ + cat. X _{TOC} = 85 %	[22]
TOC ₀ = 15 mg/L	Activated carbon Derco 15-20	20 °C, pH 7, Q _{gas} = 24 L/h, [O ₃] _{gas} = 25 mg/L, t _{test} = 2 h, Slurry SemiBatch reactor	Ads. X _{SMX} = 100 % O ₃ X _{TOC} = 28 % O ₃ + cat. X _{TOC} = 92 % Organic matter resulting from preozonation times >10 min, hardly adsorbs onto activated carbon	[22]
50 mg/L	Activated carbon Norbit GAC 1240 plus	cat. 100 mg, V _{liq} = 0.7 L, pH 4.8, Q _{gas} = 150 mL/min, [O ₃] _{gas} = 50 g/Nm ³ , t _{test} = 3 h, Slurry SemiBatch reactor	Ads. X _{TOC} = 65 % O ₃ X _{TOC} = 35 % O ₃ + cat. X _{TOC} = 45 %	[52]
50 mg/L	Commercial multi-walled carbon nanotubes (MWCN) Nanocyl3100	cat. 100 mg, V _{liq} = 0.7 L, pH 4.8, Q _{gas} = 150 mL/min, [O ₃] _{gas} = 50 g/Nm ³ , t _{test} = 3 h, Slurry SemiBatch reactor	Ads. X _{TOC} = 30 % O ₃ X _{TOC} = 35 % O ₃ + cat. X _{TOC} = 35 %	[52]
50 mg/L	CeO ₂ AC	cat. 100 mg, V _{liq} = 0.7 L, pH 4.8, Q _{gas} = 150 mL/min, [O ₃] _{gas} = 50 g/Nm ³ , t _{test} = 3 h, Slurry SemiBatch reactor	Ads. X _{SMX} = 58 %, O ₃ X _{TOC} = 34 %, O ₃ + cat. X _{TOC} = 73 %	[53]
50 mg/L	CeO ₂ /MWCNT	cat. 100 mg, V _{liq} = 0.7 L, pH 4.8, Q _{gas} = 150 mL/min, [O ₃] _{gas} = 50 g/Nm ³ , t _{test} = 3 h, Slurry SemiBatch reactor	Ads. X _{SMX} = 33 % O ₃ X _{TOC} = 34 % O ₃ + cat. X _{TOC} = 56 %	[53]
50 mg/L	CeO ₂	cat. 100 mg, V _{liq} = 0.7 L, pH 4.8, Q _{gas} = 150 mL/min, [O ₃] _{gas} = 50 g/Nm ³ , t _{test} = 3 h, Slurry SemiBatch reactor	Ads. X _{SMX} = 0 % O ₃ X _{TOC} = 34 % O ₃ + cat. X _{TOC} = 61 %	[53]
TOC ₀ = 40 mg/L	Commercial activated carbon (PAC)	cat. 2 g/L, 26 °C, pH 5, Q _{gas} = 1 L/min, [O ₃] _{gas} = 48 mg/L, t _{test} = 20 min, Slurry SemiBatch reactor	O ₃ X _{TOC} = 37 % O ₃ + cat. X _{TOC} = 78 %	[3]
TOC ₀ = 40 mg/L	FeO ₃ /CeO ₂ loaded activated carbon (MOPAC)	cat. 2 g/L, 26°C, pH 5, Q _{gas} = 1 L/min, [O ₃] _{gas} = 48 mg/L, t _{test} = 20 min, Slurry SemiBatch reactor	O ₃ X _{TOC} = 37 % O ₃ + cat. X _{TOC} = 86 %	[3]
Intermediates of 10 min ozonation of 0.0001 mol/L SMX	Activated carbon Darco 12-20 (PAC)	cat. 1 g/L, 20 °C, pH 7, Q _{gas} = 25 L/h, [O ₃] _{gas} = 20 mg/L, t _{test} = 40 min, Slurry SemiBatch reactor	Ads. X _{TOC} = 6 % O ₃ X _{TOC} = 17 % O ₃ + cat. X _{TOC} = 32 % (10 min)	[3]
50 mg/L	Treated Commercial multi-walled carbon nanotubes MWCN-HNO ₃ -N ₂ -900	cat. 100 mg, V _{liq} = 0.7 L, pH 4.8, Q _{gas} = 150 mL/min, [O ₃] _{gas} = 50 g/Nm ³ , t _{test} = 3 h, Slurry SemiBatch reactor	Ads. X _{SMX} = 55 % O ₃ X _{TOC} = 35 % O ₃ + cat. X _{TOC} = 45 %	[54]

50 mg/L	Treated Commercial multi-walled carbon nanotubes MWCN-O ₂	cat. 100 mg, V _{liq} = 0.7 L, pH 4.8, Q _{gas} = 150 mL/min, [O ₃] _{gas} = 50 g/Nm ³ , t _{test} = 3 h, Slurry SemiBatch reactor	Ads. X _{SMX} = 38 % O ₃ X _{TOC} = 35 % O ₃ + cat. X _{TOC} = 41 %	[54]
0.0003 mol/L	Fe ²⁺ -Montmorillonite	cat. 1 g/L, pH ₀ 2.88, [O ₃] _{dose} = 5 mg/min, t _{test} = 20 min, Slurry SemiBatch reactor	O ₃ + cat. X _{COD} = 97 %	[55]
50 mg/L	Magnetic Fe ₃ O ₄ nanoparticles	cat. 1 g/L, V _{liq} = 0.2 L, 25°C, [O ₃] _{dose} = 2 g/h, t _{test} = 5 min, Slurry SemiBatch reactor	O ₃ X _{SMX} = 85 % O ₃ + cat. X _{SMX} = 97 %	[56]
50 mg/L	Heteroatom doped graphene oxide PGO	cat. 1 g/L, 25 °C, pH 9, [O ₃] _{dose} = 2 g/h, t _{test} = 5 min, Slurry SemiBatch reactor	O ₃ X _{SMX} = 62 % O ₃ + cat. X _{SMX} = 99 %	[57]
10 mg/L	γ-Ti-Al ₂ O ₃	cat. 1.5 g, V _{liq} = 1 L, pH 7, Q _{gas} = 200 mL/min, [O ₃] _{gas} = 30 mg/Nm ³ , t _{test} = 1 h, Slurry SemiBatch reactor	Ads. X _{SMX} = 8 % O ₃ X _{TOC} = 26 % O ₃ + cat. X _{TOC} = 92 %	[58]
25.3 mg/L	Iron-manganese silicate oxide	cat. 0.5 g, V _{liq} = 0.5 L, pH ₀ 7, Q _{gas} = 0.4 L/min, [O ₃] _{gas} = 9.05 mg/L, t _{test} = 1 h, Slurry SemiBatch reactor	Ads. X _{SMX} = 1.8 % O ₃ X _{TOC} = 27 % O ₃ + cat. X _{TOC} = 79.8 % Adsorption of SMX intermediates at 30 min (cat. 0,1 g/L) = 17.9 %	[24]
30 mg/L SMX + 30 mg/L diclofenac	Fe-Mn-O	cat. 1 g/L, pH ₀ 5.5, Q _{gas} = 2 L/min, [O ₃] _{gas} = 10 g/m ³ , t _{test} = 2 h, Slurry SemiBatch reactor	O ₃ X _{TOC} = 44 % O ₃ + cat. X _{TOC} = 63 %	[59]

1. Experimental

1.1. Chemicals and reagents

Aluminum isopropoxide Al[OCH(CH₃)₂]₃ (Aldrich, ≥ 98%), γ-Al₂O₃ (SASOL), ethanol (Cicarelli, 99.5%), ferric nitrate nonahydrate Fe(NO₃)₃·9H₂O (AppliChem), nitric acid HNO₃ (70 %w/w, Cicarelli PA), Pluronic P123 PEG-PPG-PEG (Aldrich), sodium bisulfite NaHSO₃ (Panreac), potassium indigotrisulfonate C₁₆H₇K₃N₂O₁₁S₃ (Sigma Aldrich), sulfamethoxazole C₁₀H₁₁N₃O₃S (Sigma). Oxygen (Abelló Linde, > 99.99%). Acetic acid and acetonitrile (Panreac, HPLC grade). Milli-Q water was produced by a filtration system (Millipore, USA).

1.2. Synthesis of mesoporous alumina and Fe-alumina catalysts

Mesoporous alumina was synthesized by using an adaptation on a larger scale of the EISA methodology reported by Morris and co-workers [17,60]. The experimental procedure was detailed elsewhere [31]. Briefly, 20 g of Pluronic P123 was dissolved in 200 mL of anhydrous ethanol and stirred for 4 h (solution A). Meantime, solution B was prepared from 32 mL of nitric acid, 100 mL of anhydrous ethanol and 0.2 mol of aluminum isopropoxide. Subsequently, the two solutions were combined in one-pot and 100 mL of anhydrous ethanol was used to thoroughly transfer the aluminum isopropoxide solution. The final solution

was stirred for 5 h at room temperature. The molar ratios $[Al] : [PTZ] : [EtOH] : [HNO_3]$ in the final solution were fixed at 1 : 0.017 : 30 : 2.5. Afterwards, solvent evaporation of the sol was performed in a drying oven at 60°C for 48 h. The resulting xerogel was heat-treated at 400 °C (heating rate of 1°C/min, 4 h). The calcined samples, which were ground into powders, will be referred to as MA.

Additionally, the mesoporous alumina matrix was doped with Fe. This material was prepared by adding ferric nitrate to solution A. The other steps of the synthesis were the same as those given above. The total quantity of metal species was kept constant and the molar ratio $[Fe] : [Al]$ was adjusted to 0.064. The total iron content resulted in 4.7 wt% and the material was labeled as MA-5Fe.

1.3. Characterization

The characteristics of MA and MA-5Fe materials were determined by different techniques and the results were contrasted with a commercial alumina sample (CA). Powder X-ray Diffraction (XRD) was conducted with a PANalytical X'Pert Pro diffractometer by using $CuK\alpha$ radiation ($\lambda = 1.54056 \text{ \AA}$). The nitrogen adsorption and desorption isotherms at -196 °C were measured using a Micrometrics ASAP-2020 instrument. Prior to physisorption analysis, samples were degassed overnight at 120 °C under vacuum conditions. Transmission Electron Microscopy (TEM) was performed in a TEM JEOL 100 CX II instrument. Thermogravimetric Analysis (TGA) of the xerogel was performed with a TGA Q500 V 20.13 (TA instruments) using air atmosphere (10 °C/min). Elemental organic analysis was performed in a Thermo Scientific EA 1108 instrument. The point of zero charge (PZC) was determined by the mass titration method following the protocol reported by Preočanin and Kallay [61]. Different catalyst masses were added to aqueous solutions of different initial pH values adjusted by addition of HNO_3 or KOH . During the experiment, the pH of each solution changes gradually and once equilibrated approaches to the PZC. The ionic strength was kept constant at 0.003 mol/L and controlled by KNO_3 as background electrolyte. The experiments were performed in a closed reactor of 25 mL at room temperature and purged with N_2 . Temperature programmed desorption of pyridine (TPD-pyridine) was performed to determine acidic properties using a Pyris 1 TGA instrument (Perkin Elmer). Samples were pretreated by heating from 50 to 400 °C (10 °C/min, purged with air) to remove surface impurities. Then the samples were cooled to 120 °C and purged with N_2 , followed by the surface saturation with pyridine until constant weight, the excess of probe molecule was removed in N_2 flow for 120 min. The samples saturated with pyridine were subjected to

IG analysis by heating up from 120 to 400 °C (20 °C/min). Total iron content and leached Fe were determined by a standard colorimetric test (FerroVer®Iron Reagent, HACH) with a detection range between 0.02 to 3.00 mg/L Fe. In order to obtain the iron content in the solid sample, MA-5Fe was digested in HNO₃-HF. The reported values are the average of at least two different samples.

1.4. Catalytic ozonation tests

Catalytic ozonation of SMX was performed in a 1.5 L jacketed semibatch stirred-tank reactor using 1 L of working volume. Ozonation experiments were performed at room temperature (22 °C) and controlled by circulating water from a thermostatic bath. The initial SMX concentration was 20 mg/L and the reaction time was set in 120 min. Gas flow rate and ozone inlet concentration were kept constant at 42 L/h NTP (0 °C and 1 atm) and 10 mg/L NTP, respectively. Therefore, the applied ozone dose was 88 mg O₃/mg TOC, which is in the range of the values reported in Table 2 for SMX ozonation. Ozone was produced from dry pure oxygen by a Sander ozone generator and was injected at the bottom of the reactor by means of a T-pipe coupled to two stainless steel diffusers. The reaction volume was stirred with a magnetic stirrer (700 rpm) to ensure the good contact between the liquid and gas phases. Figure 1 shows a scheme of the ozone installation.

Ozone balance was assessed as described elsewhere [62]. Briefly, continuous measurements of ozone concentration were carried out in the gas phase at the inlet and outlet of the reactor and also in the liquid phase. The transferred ozone dose (TOD), which refers to the quantity of O₃ consumed and residual ozone dissolved in the water sample per unit of sample volume, was calculated.

Since MA and MA-5Fe have different specific surface area, the solid concentration was adjusted to have 220 m² per liter of reaction volume (c.a. 1 g/L). At selected ozonation tests, initial pH was adjusted below and above the PZC of the materials by using NaOH and HCl. In order to give a more realistic approach, different water matrices such as bottled water and a secondary effluent collected from the outlet stream of the municipal wastewater treatment plant from Gavà-Viladecans EDAR (December 2016, Barcelona) were spiked with SMX. The composition of the bottled water according to its label was: 17 mg/L bicarbonates, 1.21 mg/L Na, 0.54 mg/L Cl, 0.83 mg/L Mg, 6.3 mg/L Ca, 9.8 mg/L Si with an electrical conductivity of 237 µS/cm and a pH = 6.75. The most important chemical properties of the secondary effluent are summarized in Table 3.

Ozonation alone at different initial pH values and blank experiments were used as reference. Moreover,

adsorption contribution was measured without ozone. In these tests, single ozonation of SMX was performed during 5, 15, 30 and 60 min, the residual ozone was purged with O₂ (30 min) and the remnant TOC concentration was measured; then, mesoporous alumina was added to the reactor and the mixture was stirred under oxygen flow until no changes were detected in TOC values.

In order to confirm the repeatability of the ozonation experiments, the reaction runs were performed at least in duplicate with experimental errors below 10% in all cases.

In addition, experiments of ozone decomposition were performed in ultrapure water matrix and by using ozonation supernatants collected at 120 min. The operating conditions were set at: V = 500 mL, Q_{gas} = 21 L/h NTP, [O₃]_{gas} = 10 mg/L NTP, [solid] = 1 g/L and T = 22 °C. For ultrapure water, the liquid volume was saturated with ozone for 30 min; afterwards, the ozone generator was switched off and the solids were added to the reactor. For reaction supernatants, the ozonation of SMX (20 mg/L) was conducted for 120 min with and without MA-5Fe; afterwards, the ozone generator was switched off and residual ozone concentration was monitored without replacing the catalyst. In both cases, the initial concentration of dissolved ozone was c.a. 1.5–2 mg O₃/L. In these tests, the use of buffered systems was avoided to prevent the interaction of anions with the surface sites of the catalyst.

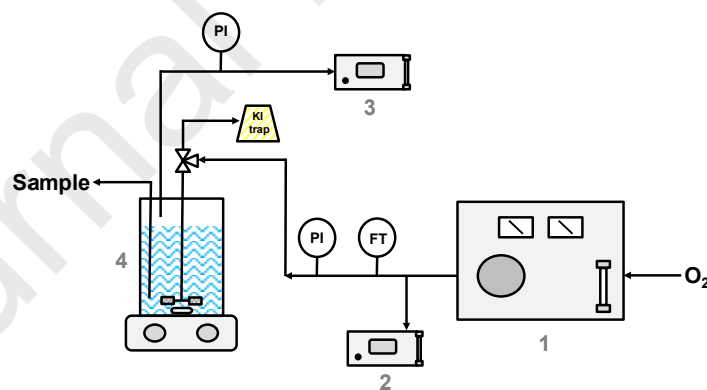


Figure 1. Scheme of the ozonation installation: 1) ozone generator, 2) inlet O₃ analyzer, 3) outlet O₃ analyzer and 4) stirred-tank reactor.

Table 3. Characterization of the municipal secondary effluent used in this work.

Parameter	Mean value
pH	7.85
TC, mg/L	38.5
TOC, mg/L	20.68

COD, mg O ₂ /L	79.5
Filtered COD, mg O ₂ /L	68.8
UVA ₂₅₄	0.156
Turbidity, NTU	0.9
Alkalinity, mg CaCO ₃ /L	346.2
Cl, mg/L	32.41
Na, mg/L	611.46
Ca, mg/L	99.34
Mg, mg/L	57.96
Total Solids, mg/L	2.36

1.5. Analytical methods

Liquid samples were periodically withdrawn and immediately quenched with 0.025 M of NaHSO₃ to remove residual ozone. Prior to analysis, all samples were filtered (RC 0.45 µm syringe filter). The reaction progress was monitored in terms of SMX concentration, Total Organic Carbon (TOC), aromaticity removal (UVA₂₅₄), ozone consumption and pH evolution.

The concentration of SMX was quantified by High Performance Liquid Chromatography (HPLC) equipped with a diode array detector (DAD) supplied by Agilent (1260 Infinity). The HPLC column was a Mediterranea Sea18 (250mm×4.6mm and 5µm size packing) and the mobile phase consisted in a solution of acetonitrile (60:40) and acidified water (acetic acid, pH 3). The wavelength of the UV detector was set at 270 nm and the flow rate kept at 1 mL/min. Under these conditions, the retention time of SMX was 4.2 min. The transformation products of SMX were identified by Liquid Chromatography-Electrospray Ionization-Time of Flight-Mass Spectrometry (LC-ESI-TOF-MS). These analyses were performed using a HPLC Agilent 1100 and the chromatographic method described above. The HPLC system was connected to an Agilent G1969A TOF mass spectrometer with an electrospray interface operating in positive ionization mode under the following conditions: injection volume, 10 µL; sample inlet flow, 0.275 mL/min; capillary voltage, 4000 V; nebulizer pressure, 30 psig; drying gas flow, 10 L/min; drying gas temperature, 325 °C; fragmentor voltage, 175 V; data acquisition, 25-1100 m/z.

TOC determination was carried out in a Shimadzu 5055 TOC-VCSN analyzer (Shimadzu, Japan).

Aromaticity was monitored in terms of ultraviolet absorbance at 254 nm [63] and measured with a UV-Vis spectrophotometer Lambda 20 (Perkin-Elmer, USA).

Ozone concentrations were measured in the gas phase by using two ozone analyzers BMT 964 BT (BMT Messtechnik GMBH, Germany) and in the liquid phase by the indigo method [64].

2. Results and discussion

2.1. Characterization results

After calcination at 400°C, all organic residues from the EISA synthesis were removed from the solids (TGA) and no crystalline phases were evidenced by XRD analysis (not shown). TEM images displayed the development of ordered mesoporous structures with narrow cylindrical channels of ca. 10nm (Figure 2). For comparative purposes, Figure 2 also includes the micrograph of a commercial alumina sample (CA), showing noticeable structural differences in relation with the synthesized MA materials. In agreement, N₂ Physisorption measurements revealed the development of mesoporous materials with a BET surface area of 263 m²/g for MA and 211 m²/g for MA-5Fe. Both samples displayed type IV isotherms and H3 hysteresis loops (Figure 3), typical from mesoporous materials [65] and a narrow pore size distribution centered on 10 nm (Table 4). However, it should be noted that the adaptation on a larger scale of the EISA procedure impacted negatively on the porosity of the MA samples, displaying significant smaller surface areas and pore volumes than expected [60]. In comparison, CA sample exhibited slightly lower BET surface area and pore volume than MA, resulting in 200 m²/g and 0.5 cm³/g respectively, with an average pore width of 7.15 nm (Table 4). Moreover, the CA physisorption isotherm showed a different shape of pore structure, type IV with H2(b) hysteresis loop (Figure 3), which might indicate a more complex pore structure, with important network effects probably related with pore blocking [65].

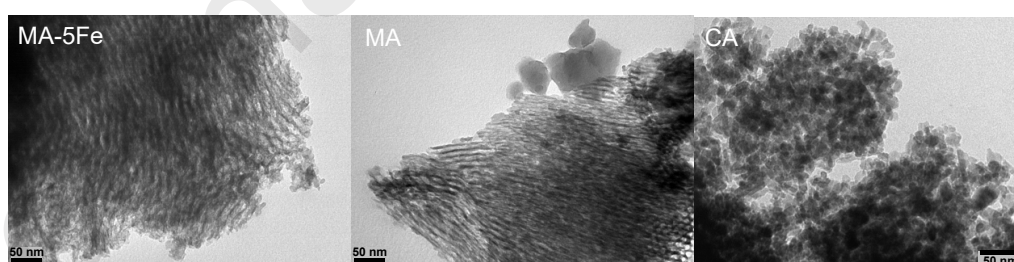


Figure 2. TEM images of synthesized mesoporous aluminas (MA) and commercial γ -Al₂O₃ (CA).

Table 4. Summary of characterization outcomes.

Sample	S _{BET} (m ² /g)	V _{pore} (cm ³ /g)	d _{pore} (nm)	PZC	Acid sites (mmol/g)	Pyridine desorption temperature (°C)
MA	263	0.79	10.2	7.7	0.130	235
MA-5Fe	211	0.55	9.67	7.5	0.200	235
CA	200	0.50	7.15	7.6	0.097	227

Surface reactivity is determined by structural and coordinative arrangement around the surface of the metal centers. The point of zero charge (PZC) is a central concept in the adsorption of charged species and its position defines the affinity of the solid surface to the ionic species [66]. The PZC values of MA and MA-5Fe resulted in 7.7 and 7.5, respectively; which is consistent with those reported in the literature for similar metal oxide systems [14,66]. This means that during the ozonation tests, alumina surface will be positively charged and will adsorb/attract anions and negatively charged ligands from effluents with a $\text{pH} < \text{PZC}$.

Metal oxides' reactivity is determined by their acidity and basicity. Hydroxyl groups formed at the surface behave as Brønsted acid sites, whereas Lewis acids and Lewis bases are sites located on metallic cations and coordinatively unsaturated oxygens, respectively [14]. The acidity of MA samples was determined by TPD of pyridine (Table 4). The measurements showed that Fe incorporation increased the quantity of acid sites of MA. By contrast, the CA sample showed a lower concentration of surface acidic sites. According to the pyridine desorption temperature, MA and MA-5Fe showed a slightly higher acidic strength than CA, which might enhance the surface reactivity of the synthesized materials [31].

From these results, MA and MA-5Fe displayed enhanced surface and structural properties in relation with a commercial alumina, which make them promising candidates for the removal of organic molecules from water. The availability of well-defined cylindrical channels might improve the diffusion of organic substrates. Furthermore, the preparation methodology of MA-5Fe promotes both an enhanced anchorage of Fe (in contrast with wet impregnation procedures) and its homogeneous distribution on the alumina network.

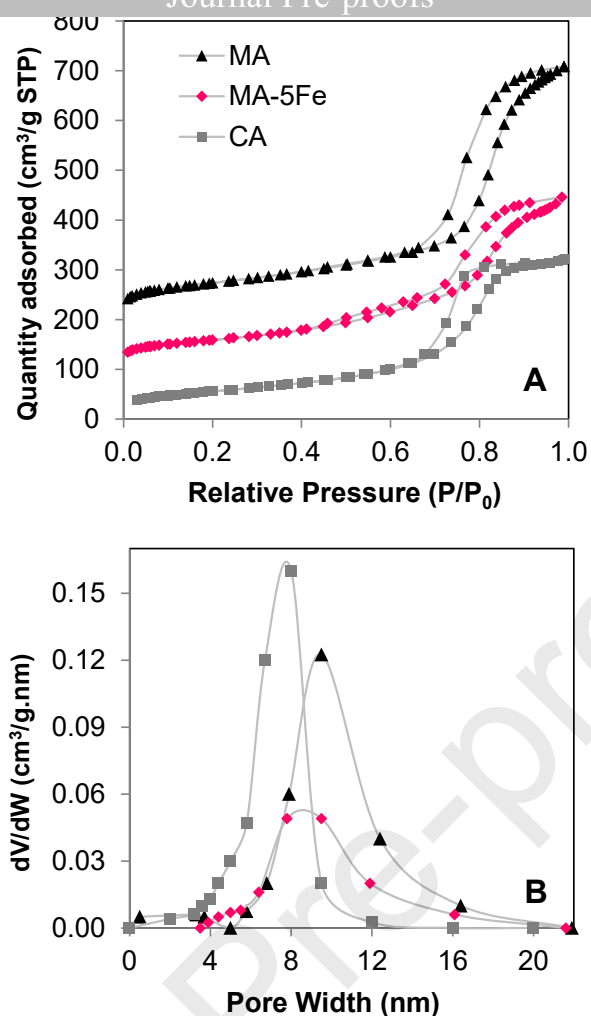


Figure 3. N₂ Physisorption results: isotherms at -196 °C (A) and pore size distribution (B).

2.2. Ozonation of SMX

2.2.1. Single ozonation

Ozonation alone carried out at different pH showed a fast disappearance of SMX and aromatic compounds (Figure 4). After the first 30 min, almost total conversion of SMX was reached with more than 80% conversion of aromatics (corresponding TOD = 116 mg/L). Ozone selectively attacks activated aromatic rings or double bonds of SMX. In fact, the amino group (-NH₂) is an electron donating group, which activates the aromatic ring towards ozone attack, by increasing its electronic density [52,67]. As observed by other authors, SMX oxidation was nearly independent of pH (the direct rate constant of the SMX–ozone reaction varies between 2.65×10^5 and 4.65×10^5 M/s for pH 2 and 9, respectively) [22,68]. Moreover, the ozone concentration in the liquid phase was negligible during the first 15–20 min (Figure 5), which indicates that SMX molecules reacted in the liquid film close to the gas-liquid interface. Therefore, ozone, once dissolved in water, was totally depleted by reacting with SMX and, most likely, first unsaturated

intermediates [22]. Without adjustment, pH decreased from an initial value of 4.8 to a plateau of 5.5 due to the formation of acid intermediates. This tendency was repeatedly observed in spite of the adjustment of initial pH performed in some of the tests (Figure 4-B). Experiments carried out under controlled pH conditions did not affect the rate of SMX and aromaticity decaying. Concerning TOC removal, single ozonation allowed a mineralization level of 26% under acidic conditions ($\text{pH}_0 = 4.8$); whereas under controlled neutral pH 6.7–7 and $\text{pH}_0 = 9.4$, TOC conversion increased slightly to 35 % (Figure 4-C) due to an enhancement in O_3 decomposition into hydroxyl radicals [52].

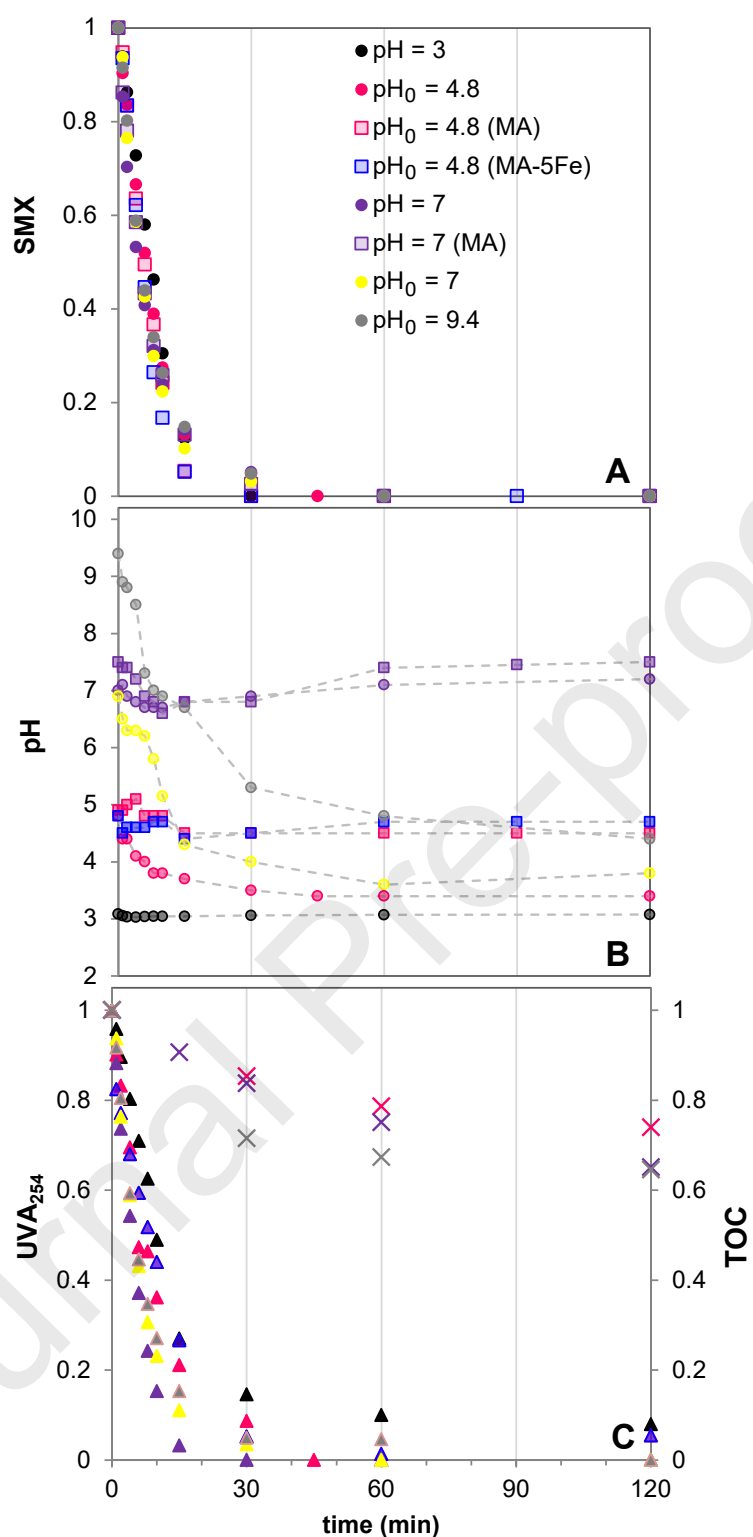


Figure 4. Ozonation of sulfamethoxazole reported as dimensionless values of SMX, UVA₂₅₄ and TOC. Effect of pH: A) SMX decomposition; B) pH profiles and C) TOC removal (×) and UVA₂₅₄ (Δ). (Operating conditions: $Q_{\text{gas}} = 42$ L/h NTP, $[O_3]_{\text{gas}} = 10$ mg/L NTP, $[SMX] = 20$ mg/L, $T = 22$ °C).

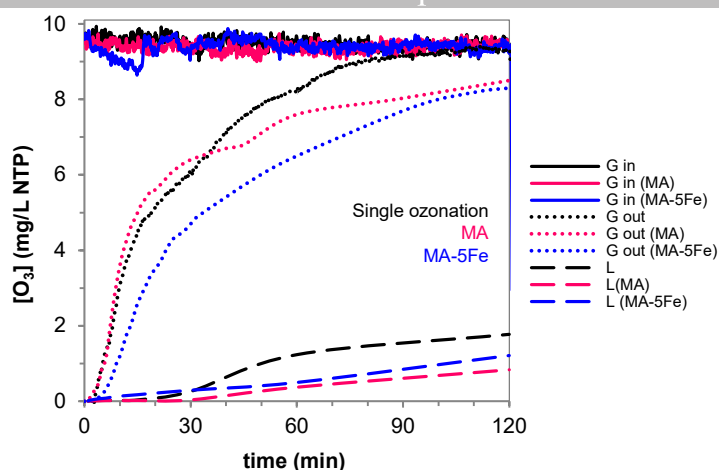


Figure 5. Ozone profiles for single ozonation and ozonation with MA and MA-5Fe. (Operating conditions: $Q_{\text{gas}} = 42$ L/h NTP, $[\text{O}_3]_{\text{gas}} = 10$ mg/L NTP, $[\text{SMX}] = 20$ mg/L, $T = 22$ °C, $\text{pH}_0 = 4.8$).

2.2.2. Ozonation with mesoporous alumina and Fe-doped alumina

During ozonation tests with MA and MA-5Fe, the measured values of SMX, UVA_{254} and initial O_3 liquid concentration profiles (15–30 min) showed similar results to those observed for single ozonation (Figure 4 and 5). This indicates that under the operating conditions tested, oxidation of SMX and aromatics is mostly a consequence of direct ozone reactions since SMX hardly adsorbs on MA surface (< 10 % adsorption). In addition, as shown in Fig. 5, the concentration of ozone in the aqueous phase is negligible during the first 30 min, therefore, ozone-promoted surface reactions cannot develop because ozone does not reach the liquid film close to the water–solid interface [22]. However, TOC evolution does differ between single ozonation and tests performed in the presence of the alumina materials (Figure 6). Without pH adjustment ($\text{pH}_0 = 4.8$), TOC removal increased from 26 % (single ozonation) up to 81 % with MA and 86% with MA-5Fe. At neutral pH, the reaction's performance decreased ($X_{\text{TOC}} = 65\%$) due to the zero surface charge, which attracted fewer anions and negatively charged ligands. In all cases, ozonation with MA-5Fe did not register iron leaching. From these results, it can be seen that the addition of MA or MA-5Fe increases almost equally the TOC removal indicating that under the conditions tested the ferric species do not have a significant contribution in organic matter elimination.

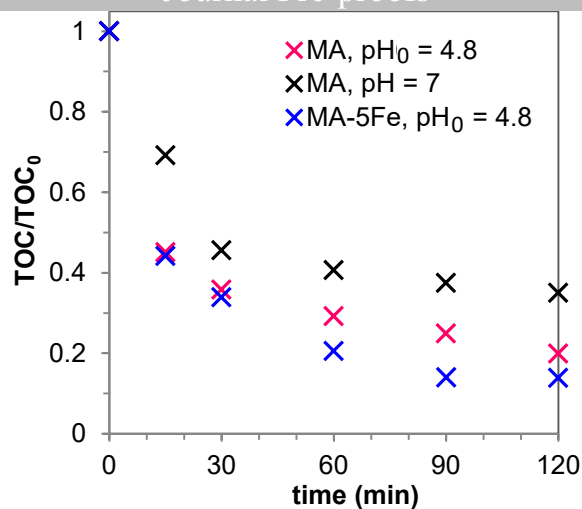


Figure 6. Ozonation with MA and MA-5Fe. (Operating conditions: $Q_{\text{gas}} = 42$ L/h NTP, $[\text{O}_3]_{\text{gas}} = 10$ mg/L NTP, $[\text{SMX}] = 20$ mg/L, $T = 22$ °C, $[\text{solid}] \approx 1$ g/L).

Regarding pH profiles, the addition of mesoporous alumina buffered the pH of the reaction volume due to a compensation effect between the formation of acidic intermediates and the protonation of the surface due to operation below PZC (Figure 4-B). Accordingly, it is clearly seen from the ozone profiles displayed in Figure 5 that the presence of solids contributes to a drop in the ozone concentration in the outlet gas stream and in the liquid phase. The same trend was repeated in a blank test with MA plus O_3 in the absence organics, where the final pH approached to the PZC. The final TOD values (120 min) for experiments performed at acid pH resulted in 225 mg/L for MA and 239 mg/L for MA-5Fe, whereas for single ozonation the measured TOD was only 159 mg/L. On the other hand, at neutral pH, ozonation with MA reached a TOD of 297 mg/L. Therefore, the trend in TOD values and the ozone profiles displayed in Fig. 5 might suggest the ozone decomposition in the presence of mesoporous alumina. Unlike the results reported by Nawrocki and Fijolek [28] about the presence of sodium impurities on commercial aluminum oxides, this can be discarded here due to the high purity of the synthesis procedure.

2.2.3. Ozone decomposition with and without mesoporous alumina

The activity of catalysts in the ozonation process is frequently attributed to the decomposition of ozone into reactive oxygen species (ROS). To confirm this effect, experiments of ozone decomposition were performed in ultrapure water matrix (UW, pH = 6) and by using reaction supernatants collected at 120 min (single ozonation and catalytic ozonation with MA-5Fe, pH = 4.5). In general, the pH was not adjusted except for

the test carried out with the supernatant of single ozonation (SSO120), whose pH was adjusted to 4.5 (5 M, NaOH) to equalize the pH of the supernatant of catalytic ozonation with MA-5Fe (SCO120). Figure 7 shows the results of these tests.

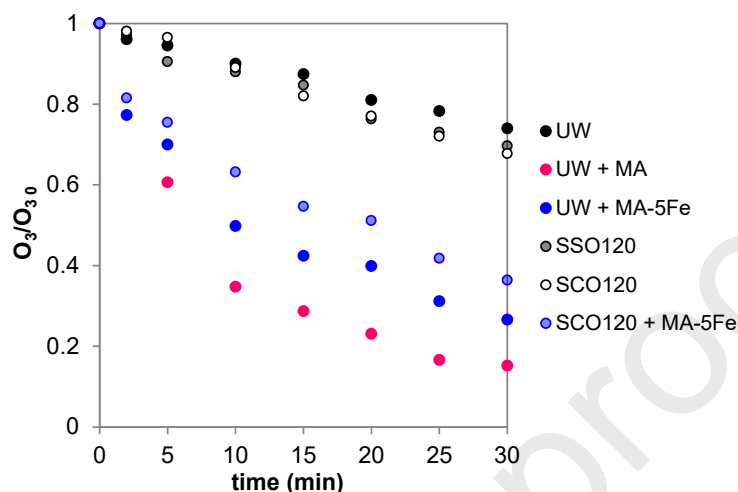


Figure 7. Evolution of dimensionless remaining ozone concentration with time during its decomposition in different water matrices (UW: ultrapure water, SSO120: supernatant of single ozonation collected at 120 min and SCO120: supernatant of catalytic ozonation collected at 120 min) in the absence and presence of MA and MA-5Fe (operating conditions: $V = 500$ mL, $[O_3]_{liq} = 1.5\text{--}2$ mg/L, $[solid] = 1$ g/L and $T = 22$ °C).

The presence of mesoporous alumina notably increased the decomposition rate of O_3 . This result is in agreement with previous findings [25,69] and indicates that reactive oxygen species (such as $\bullet OH$) may be generated in catalytic ozone decomposition with ordered mesoporous alumina. The higher ozone decomposition obtained with MA, in relation to MA-5Fe, can be attributed to its higher surface area. Moreover, the decomposition profiles also evidenced that ferric species do not enhance the ability of MA to decompose O_3 . The decrease in MA-5Fe performance in the test carried out with the reaction supernatant (SCO120 + MA-5Fe), in comparison to ultrapure water (UW + MA-5Fe), might be assigned to the partial blockage of surface sites due to the adsorption of organics and/or the higher pH of the blank test performed in UW (pH = 6).

After centrifugation of the solid, the supernatant of the catalytic ozonation test was saturated with ozone (SCO120) and ozone decomposition was evaluated. In this case, the evolution of residual ozone was similar

to the one obtained for SSOT20 which proves that the material does not release impurities to the reaction media.

2.2.4. Identification of intermediates and degradation pathway of SMX

Primary degradation products of SMX were separated and identified by liquid chromatography coupled to a time of flight mass spectrometer (LC-TOF-MS). Table 5 provides a summary of the six intermediates (C1-C6) identified within the first 30 min of treatment by single ozonation and ozonation with MA-5Fe without pH adjustment. The strategy of identification was to explore the transformation products previously found in the literature [70–72]. For this, the characteristic signals at the extracted ion chromatograms (EIC) of the suspected ions to be present were examined (Figures S1-S7 in Supporting Information). Structure assignment was based on the accurate mass measurements provided by the TOF analyzer which allows obtaining the elemental composition of the protonated molecules and ion fragments with high accuracy (<5 ppm error). In addition, the collected samples were immediately quenched with sodium bisulfite to prevent possible losses of intermediates; thus, the presence of sodium adducts, in addition to protonated molecules and ion fragments, was expected.

First, it was found a fragmentation of SMX (m/z 254 for $[M+H]^+$) according to that reported in the literature. The ion fragments displayed in Table 5 indicate the preferential breakdown of SMX at the sulfonamide bond (S–N) followed by the loss of the SO_2 group and the rearrangement of the aminobenzene moiety. The appearance of characteristic fragments may indicate the prevalence of specific parts of the original molecule, suggesting that the transformation takes place in another part of the molecular structure [71]. Second, compounds C1, C2 and C3 were produced at the beginning of the reaction (the first collected sample) and were related to the formation of hydroxylated derivatives. C1 (m/z 270.0545 for $[M+H+16]^+$), whose elemental composition ($C_{10}H_{12}N_3O_4S$) has one oxygen atom more than the parent compound, represents the hydroxylation of the benzene ring. The position of the hydroxyl group was confirmed by the presence of the ion fragment at m/z 99.057, which indicates that the isoxazole ring remained unchanged. In spite of this, the presence of C1 isomers cannot be discarded, consistently with the addition of a hydroxyl radical at different positions of the SMX structure. Further oxidation of mono-hydroxylated intermediates yielded the di-hydroxylated compound C2 (m/z 271.0374), related to the hydroxylation of the isoxazole ring and the

substitution of the amino group by an OH group in the benzene ring. Another di-hydroxylated compound (C3) was identified at m/z 288.0641, which involved the oxidation of the double bond C=C at the isoxazole ring. Further oxidation led to the cleavage of the sulfonamide bond with the formation of lower molecular weight organic compounds, C4 (m/z 190.0167) and C5 (m/z 99.057). Compound C4 corresponded to a hydroxyl-derivative of sulfanilic acid (not identified in the samples treated by single ozonation), 4-(hydroxyamino)benzenesulfonic acid [72]. C5 was identified as 3-amino-5-methylisoxazole, originated by the hydrolysis of the sulfonamide bond. In particular, the use of sodium bisulfite for ozone quenching led to co-elution problems with this by-product; however, the presence of its typical ion fragment at m/z 72.0441 confirmed its formation. It was also identified a transformation product that has not been previously reported in the literature (C6), and proposed a tentative structure. Its empirical formula ($C_{10}H_{12}N_3O_7S$ at m/z 318.0398) suggests that this product might arise from the subsequent oxidation of C3, through oxidation of the amine group at the benzene ring. This transformation was proposed in previous studies that report the formation of nitrobenzene after the ozonation of aniline at acid pH [73] and the formation of nitro-SMX as primary degradation product of SMX ozonation [55,68,74].

In summary, beyond 15-30 min of ozonation treatment none of these transformation products were identified confirming its complete removal. At initial stages, SMX and aromatic intermediates disappeared leaving compounds which are refractory towards O_3 alone. Therefore, the organic matter present in the effluent will be mainly due to unsaturated organic compounds and at last due to refractory carboxylic acids, which are also biodegradable compounds [67]. In agreement with the results, Shahidi and co-workers studied the ozonation of SMX with Fe^{2+} -montmorillonite and suggested that ozonation of SMX starts mainly via amino group hydroxylation, isoxazole ring di-hydroxylation, benzene ring hydroxylation combined with amino group oxidation and isoxazole ring separation, to form benzoquinone. The opening of the benzoquinone ring yielded muconic and maleic acids. Further oxidation of these acids generated glyoxal and oxalic acid [55]. The authors reported that oxalic acid accumulated at longer reaction times reflecting its lower reactivity. Gonçalves et al. studied the oxidation intermediates and by-products of SMX from catalytic ozonation with carbon materials. The authors identified 3-amino-5-methylisoxazole and p-benzoquinone as primary degradation products; whereas, oxamic, oxalic, pyruvic and maleic acids were detected as refractory final oxidation products [52]. Likewise, Beltrán et al. [75] studied the oxidation of SMX through ozonation and

photocatalytic processes and identified maleic and oxalic acid as main reaction intermediates. Hence, special attention should be paid to the ozonation of these refractory compounds, since the addition of a solid material contributes mainly to their removal.

Table 5. Accurate mass measurements found by LC-ESI(+)-TOF-MS spectra of protonated SMX and its degradation products.

Compound	Retention time (min)	Chemical formula	Experimental mass (m/z)	Probable reaction involved	O ₃ + MA-5Fe Reaction time (min)	O ₃ Reaction time (min)	Structural formula	Reference
SMX	4.226	C ₁₀ H ₁₂ N ₃ O ₃ S	254.0596	None	1, 2, 4, 6, 8, 10, 15	1, 2, 4, 6, 8, 10, 15		[70–72]
		C ₆ H ₆ NO ₂ S	156.0121					
		C ₆ H ₆ NO	108.0442					
		C ₄ H ₇ N ₂ O	99.0562					
		C ₆ H ₇ N	93.0566					
		C ₆ H ₆ N	92.0498					
		C ₁₀ H ₁₁ N ₃ NaO ₃ S	276.0412					
C ₂₀ H ₂₂ N ₆ NaO ₆ S ₂	529.0933							
C1	3.852	C ₁₀ H ₁₂ N ₃ O ₄ S	270.0545	Benzene ring hydroxylation	1, 2, 4, 6, 8, 10	1, 2, 4, 6, 8		[71,72]
		C ₁₀ H ₁₁ N ₃ NaO ₄ S	292.0432					
		C ₄ H ₇ N ₂ O	99.057					
C2	3.510	C ₁₀ H ₁₁ N ₂ O ₅ S	271.0374	Isoxazole ring hydroxylation and amino group substitution	1, 2, 4, 6, 8, 10, 15	1, 2, 4, 6, 8, 10, 15		[70]
		C ₁₀ H ₁₀ N ₂ NaO ₅ S	293.0219					
C3	2.747	C ₁₀ H ₁₄ N ₃ O ₅ S	288.0641	Isoxazole ring di-hydroxylation	2, 4, 6	1, 2, 4		[68,68,70,71]
		C ₁₀ H ₁₂ N ₃ O ₅ S	286.0484					
		C ₁₀ H ₁₀ N ₃ O ₅ S	284.0346					
		C ₁₀ H ₁₂ N ₃ O ₄ S	270.0543					
C4	2.291	C ₆ H ₈ NO ₄ S	190.0167	Aminophenylsulfone scission and amino group hydroxylation	2, 4, 6	ND		[72]
C5	3.114	C ₄ H ₇ N ₂ O	99.0559	Isoxazole ring scission	4, 6, 8, 10, 15	4, 6, 8, 10, 15, 30		[58,68,70–72]
		C ₃ H ₆ NO	72.0449					
C6	2.824	C ₁₀ H ₁₂ N ₃ O ₇ S	318.0398	Nitration of the amine group	ND	8, 10, 15		This work
		C ₁₀ H ₁₂ N ₃ O ₆ S	302.0449					
		C ₁₀ H ₁₄ N ₃ O ₅ S	288.0643					
		C ₁₀ H ₁₂ N ₃ O ₄ S	270.0547					

2.2.5. Role of iron

In order to evaluate the role of Fe in ozonation, reaction experiments with homogeneous iron were performed using 10 mg/L of Fe³⁺ (from Fe(III) nitrate nonahydrate). According to other authors, ozonation with homogeneous catalysts proceeds via two major mechanisms: i) decomposition of ozone by means of active metal ions present in aqueous solution generating free hydroxyl radicals and ii) formation of complexes

between the catalyst and organic molecules such as carboxylic acids and subsequent oxidation of the complex by ozone [12].

The activity of homogeneous Fe-type catalysts has been reported in several studies under strict reaction conditions, such as pH 2–3 [33,76]. Therefore, three ozonation experiments were performed at pH 3: single ozonation, O₃ plus MA-5Fe and O₃ plus Fe³⁺. Figure 8 shows the results for the ozonation with homogeneous ferric ions. At acid pH, the performance of single ozonation and O₃ plus MA-5Fe (not shown) was comparable to the results described above. Again, the homogeneous Fe³⁺ did not influence SMX degradation and its removal was due to direct ozone attack. As regards TOC removal, the addition of ferric species achieved a conversion of 41% increasing in 57% the mineralization yielded by sole ozonation ($X_{\text{TOC}} = 26\%$).

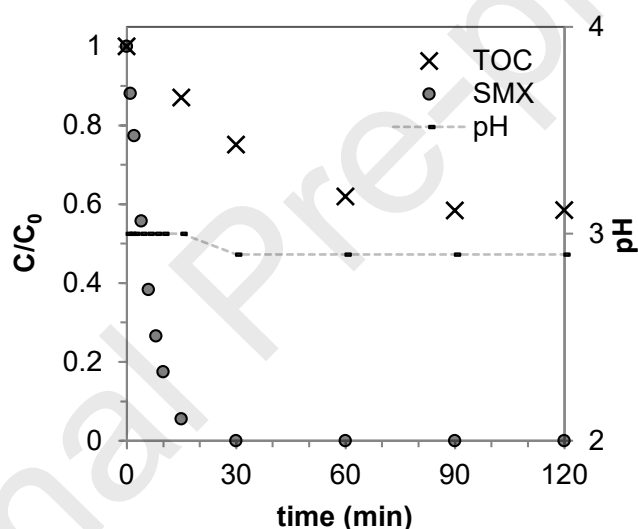


Figure 8. Ozonation with homogeneous Fe³⁺ reported as dimensionless values of SMX and TOC (operating conditions: $Q_{\text{gas}} = 42$ L/h NTP, $[O_3]_{\text{gas}} = 10$ mg/L NTP, $[SMX] = 20$ mg/L, $T = 22$ °C, $[Fe^{3+}] = 10$ ppm).

Most studies on Fe-based catalysts registered its leaching even at trace level [10,33,76–78]. Beltrán et al. [33] reported the partial leaching of Fe during the ozonation of oxalic acid with Fe₂O₃/Al₂O₃. The authors concluded that both the heterogeneous and homogeneous reactions develop simultaneously in a typical test of heterogeneous catalytic ozonation. Accordingly, the results obtained may indicate that the synthesis procedure of MA-5Fe promoted an enhanced iron anchorage. Therefore, the lack of Fe-leaching might suggest the absence of a combined homogeneous-heterogeneous catalytic mechanism with the ferric species.

In agreement with ozone decomposition tests, the catalytic contribution of the supported ferric species was not significant in relation to bare mesoporous alumina.

2.2.6. Assessment of adsorption contribution

A new set of experiments was proposed in order to understand the role of MA in the ozonation of SMX. In these tests, the pollutant was pre-oxidized by single ozonation (30 min, no pH adjustment) to be transformed into reaction intermediates which are more refractory towards ozone than SMX itself. Afterwards, the single ozonation supernatant ($\text{TOC}_0 = 8.1 \text{ mg/L}$) was employed in experiment A and B. In experiment A, the ozone generator was shut off and the reactor was bubbled with O_2 to purge the ozone traces in the reaction media (30 min). Later, MA was added to the reactor under oxygen bubbling and the test continued for 90 min. In experiment B, MA was added to the reactor under ozone/oxygen bubbling and the ozonation test continued for 90 min. At the end of each test, MA was filtered and reused in four consecutive cycles without pretreatment. Black columns in Figure 9 display the percentage of TOC removal in the last ninety minutes of these experiments. For comparative purposes, single ozonation performance was also included.

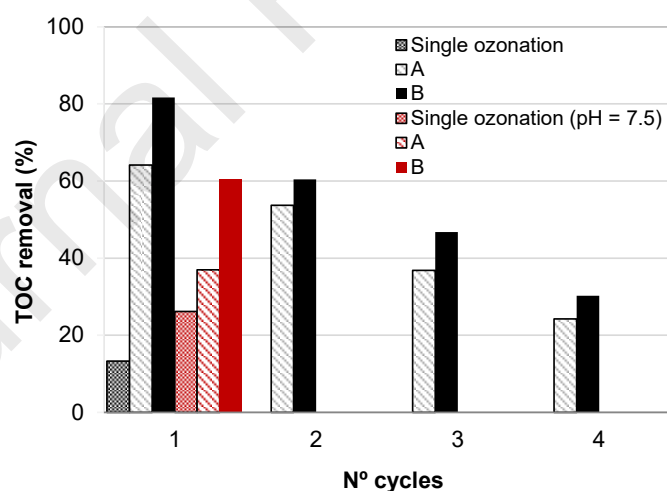


Figure 9. Adsorption and catalytic ozonation of by-products. Experiment A: Adsorption of by-products on MA under oxygen flow; Experiment B: Catalytic ozonation of by-products with MA. Black columns represent tests without pH adjustment ($\text{pH}_0 = 3.6$) while the reds are at $\text{pH} = 7.5$ (operating conditions: $Q_{\text{gas}} = 42 \text{ L/h NTP}$, $[\text{O}_3]_{\text{gas}} = 10 \text{ mg/L NTP}$, $[\text{TOC}]_0 = 8.1 \text{ mg/L}$, $T = 22 \text{ }^\circ\text{C}$, $t = 90 \text{ min}$).

From these results, the ozonation of SMX with ordered mesoporous alumina seems to be the sum of both effects: ozonation alone and adsorption contribution. After each cycle, TOC removal diminished for both experiments. This indicates that under the chosen operating conditions, MA deactivated probably due to adsorption of by-products. To prove this more directly, MA-5Fe was used in a first cycle of Experiment A and reused in a regular catalytic ozonation test. The catalyst used in the adsorption of by-products achieved a final TOC removal of 58%, which means a reduction of almost 30% compared to the fresh catalyst (Figure S8). As was confirmed in a previous work [31], MA behaves as a strong adsorbent, which can be interpreted in terms of the ligand exchange model where anions and organic acids replace the hydroxy groups on the Al_2O_3 surface [23,31]. Therefore, the decreased TOC removal was due to a smaller number of available Al-OH sites owing to the irreversible chemisorption of carboxylates [27].

The formation of such surface complexes depends on the pKa values of the acids, the electrical surface properties of the material, the surface affinity towards ligands, as well as other parameters [19,23]. Taking into account these variables, a new series of tests was performed aiming to minimize the adsorption contribution. Then, experiments A and B were repeated with the pre-ozonized supernatant adjusted to a pH = 7.5 (~ PZC of the material). Under this operating condition, the surface charge approaches to a neutral value and the dissociation of acid by-products is increased. Red columns in Figure 9 show the results of these tests. As expected, the TOC removal by adsorption decreased from 64 % at acid pH to 33 % at neutral pH while single ozonation performed slightly better at higher pH (26 % TOC removal). This trend was also confirmed by elemental organic analysis evidencing an increase of 0.7 wt% and 0.3 wt% C after the first cycle of use (Experiment B – 1st cycle in Figure 9) at acid and neutral pH, respectively. Again, the reaction intermediates were strongly adsorbed on MA surface sites and the catalytic effect could not be discriminated. Moreover, the by-products distribution changed along the reaction time, with the generation of reaction intermediates with different binding affinity towards alumina. Then, additional experiments were performed with reaction supernatants collected at different reaction times. In these tests, single ozonation was carried out for 5, 15, 30 and 60 min; afterwards, the reaction volume was purged with oxygen (30 min) and MA-5Fe was added to the reactor. The experiment was continued until no

changes were detected in TOC values. As can be observed from Figure 10, the adsorption of organic matter was more significant as reaction time advanced. Finally, these sequential tests (single ozonation + by-products adsorption) were extended to a third additional step of catalytic ozonation. For this, when the adsorption step achieved a stable TOC value, the reaction media was again bubbled with the ozone/oxygen mixture. In all cases, a slight increase in TOC removal in the range of 2–6% was registered, which suggests that under the conditions tested the catalytic effect is low.

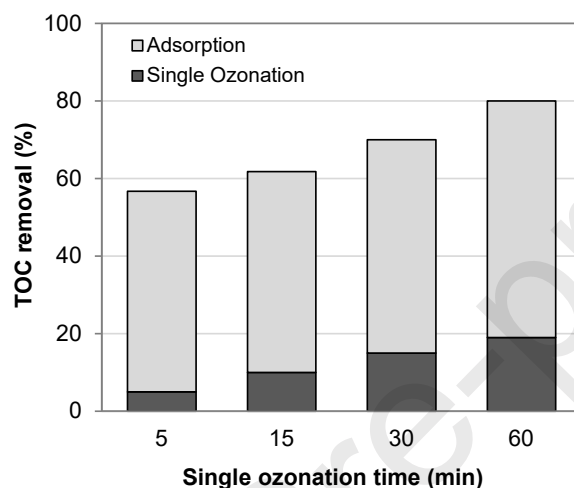


Figure 10. Single ozonation carried out during 5, 15, 30 and 60 min followed of adsorption of by-products with MA-5Fe (operating conditions: $Q_{\text{gas}} = 21$ L/h NTP, $V = 500$ mL, $[O_3]_{\text{gas}} = 10$ mg/L NTP, $[SMX] = 20$ mg/L, $T = 22$ °C, $pH_0 = 4.8$, $[\text{solid}] = 1$ g/L).

From these results, the adsorption of by-products seems to be the predominant mechanism for the removal of organic matter. Under the chosen operating conditions, mesoporous alumina behaves as a strong adsorbent while ozone enhances the removal of organics by increasing the molecular polarity of oxidized compounds, which are more feasibly adsorbed on the surface sites of MA [8]. Nevertheless, the development of a catalytic mechanism cannot be discarded since the materials are capable of decomposing ozone.

2.2.7. Reusability of MA

In order to regenerate the material, the spent sample was treated by direct ozonation in gas phase. Under this configuration, the absence of water avoids the problem of ozone solubility and mass transfer restrictions.

This set-up is also advantageous for the continuous treatment in a fixed-bed reactor; when the catalyst/adsorbent is exhausted, the column can be drained and dried with ambient or heated air. To regenerate MA, the worn sample (Experiment B – 4th cycle in Figure 9) was placed in a U-shaped fixed-bed reactor and fed with 8 mg/min of O₃ during 30 min at 25 °C.

Afterwards, the restored solid was tested following the procedure of experiment B as described before. In this new cycle, the activity of MA was partially recovered achieving a final TOC removal of 65 %. These results demonstrate that ozone can effectively regenerate alumina via oxidizing the adsorbed reaction intermediates. Nevertheless, to fully recuperate the performance of fresh MA, further studies are required to optimize the regeneration step in terms of ozone dose and exposure time.

2.2.8. Mechanism discussion of ozonation with aluminum oxides

Several mechanisms of catalytic ozonation with alumina have been proposed in the existing literature, though they remain controversial and some of them are contradictory. There are three major mechanisms for the ozonation with heterogeneous catalysts: i) chemisorption of O₃ on the catalyst surface leading to the formation of reactive species and its further reaction with non-chemisorbed organic molecules; ii) chemisorption of organics on the catalyst surface and its further reaction with dissolved ozone and iii) chemisorption of both ozone and organics on the catalyst surface and its further interaction. The catalytic effect is present when the contribution of ozone plus the catalyst is higher than a combined effect of adsorption (main pollutant and its oxidation by-products) and ozonation alone carried out at the same pH [21].

Summarizing the best documented literature cited in Table 1, it can be seen that the comparison among different works is difficult due to the wide range of operating conditions applied as well as the experimental set-ups. Among them, Pocostales et al. [39] studied the ozonation of Diclofenac, SMX and 17-ethynylstradiol with commercial γ -Al₂O₃ and Co₃O₄/Al₂O₃ in a semi-batch fixed bed reactor by using a solid to liquid ratio of 20 g/L and an ozone dose of 2000 mg/L·h ($[O_3]_{\text{gas}} = 20$ mg/L, $Q_{\text{gas}} = 25$ L/h, $V_{\text{liq}} = 0.25$ L and a mass ratio of solid : TOC = 1266). The authors found that the adsorption of carboxylates was considerable in the case of alumina. The presence of Co improved in 10% the final TOC removal in relation

with bare alumina at pH 5–6 and leached Co(II) was registered at trace levels. It was speculated that catalytic activity was due to ozone chemisorption and its further decomposition into free radicals and/or the adsorption of organics and its further reaction with ozone. Al-Hayek et al. [79] explored the catalytic effect of commercial alumina supported Fe(III) for the ozonation of phenol and its ozonation by-products. The ozone installation was a semi-batch fixed bed reactor packed with a catalyst load of 8–11.4 g/L, with an ozone dose of 48 mg/L·h ($O_3 = 1.75$ mmol/h, $Q_{\text{gas}} = 45$ L/h, $V_{\text{liq}} = 1.75$ L and solid : TOC = 230556). The catalytic ozonation of phenol achieved up to 90% of TOC removal with the Fe-doped catalyst. Unfortunately, the pH evolution along the reaction time was not specified, neither the percentages of TOC removal achieved by adsorption or the occurrence Fe leaching. The authors reported the adsorption of polar by-products such as maleic, oxalic and formic acids and speculated that the high TOC reduction was due to three reactions: 1) adsorption of reagents or reaction intermediates on alumina; 2) hydrogen peroxide formation and subsequent decomposition leading to formation of free radicals and 3) ozone decomposition at the Fe(III) sites to form species more reactive than O_3 itself. Ernst et al. [23] studied the ozonation of several carboxylic acids with commercial aluminas by using batch experiments and a semi-batch pilot reactor loaded with catalyst concentrations in the range of 20–50 g/L and an ozone dose of 960 mg/L·h ($[O_3]_{\text{gas}} = 50$ mg/L, $Q_{\text{gas}} = 100$ L/h, $V_{\text{liq}} = 5.2$ L and solid : TOC = 833–3125). The authors distinguished between adsorptive and reaction processes in the batch tests. In particular, the ozonation of succinic acid performed at the same conditions with two different commercial aluminas (similar specific surface area, but different crystalline structure, porosity and PZC) achieved very different TOC removals. Moreover, the ozonation of succinic acid was evaluated in a pilot-scale reactor reaching up to 90% of TOC removal; unluckily, the adsorption contribution with this material was not assessed. The authors suggested that the higher oxidation performance with alumina was due to the interaction between ozone and surface OH-groups. Also, they suggested that adsorption of organics would not be necessary to provide the catalytic effect and may be detrimental to catalytic activity. Beltrán et al. [33] studied the ozonation of oxalic acid with Fe(III) and Fe_2O_3/Al_2O_3 . The catalyst was prepared via impregnation of Fe(III) nitrate onto a commercial alumina and the ozonation tests were performed in a semi-batch reactor by using a catalyst concentration of 1.25 g/L and an ozone dose of 900 mg/L·h ($[O_3]_{\text{gas}} = 30$ mg/L, $Q_{\text{gas}} = 24$ L/h, $V_{\text{liq}} = 0.8$ L and solid : TOC = 6250). In a

blank test, the authors verified that the catalyst does not decompose ozone suggesting the material was inert towards ozone. In addition, Al_2O_3 did not show catalytic contribution and the catalyst did not adsorb oxalic acid. It was proposed that the ozonation mechanism likely develops through the formation of iron-oxalate complexes (homogeneous leached Fe and heterogeneous ferric species) that further react with O_3 without the production of hydroxyl radicals. Keykavoos et al. [26] studied the ozonation of bisphenol A with commercial alumina (1 g/L) in a semi-batch reactor by using $[\text{O}_3]_{\text{0liq}} = 4.5 \text{ mg/L}$ and a ratio of solid : TOC = 127. On one hand, blank experiments confirmed that alumina did not decompose or adsorb ozone in the absence of organics. On the other hand, the authors attributed the benefit of using alumina to both the catalytic interaction with ozone and the adsorption of acidic reaction by-products. Unfortunately, the evolution of pH was not shown. Additionally, the reusability of alumina was evaluated in adsorption and catalytic ozonation tests concluding that, without ozone, the material loses its activity due to chemisorption of by-products; whereas, in the ozonation tests, the adsorbed organics are oxidized by O_3 retaining the catalyst activity. Vittenet et al. [27] studied the ozonation of 2,4 dimethylphenol with commercial mesoporous alumina. The ozonation tests were performed in a slurry semi-batch reactor by using a catalyst concentration of 1–5 g/L and an ozone dose of 53.3 mg/L·h ($[\text{O}_3]_{\text{gas}} = 2 \text{ mg/L}$, $Q_{\text{gas}} = 40 \text{ L/h}$, $V_{\text{liq}} = 1.5 \text{ L}$ and solid : TOC = 26–130). The advantages of using alumina were assigned to two phenomena: its ability to adsorb acids by-products and its capacity to generate $\bullet\text{OH}$ radicals at acid pH. According to the authors, the adsorption of carboxylates occurs via ligand exchange with the surface Al-OH groups; however, its contribution was difficult to assess from individual adsorption tests with oxalic, formic and acetic acids. In the long term, the irreversible chemisorption of carboxylates decreased the TOC removal due to a decreased amount of available Al-OH sites. Finally, Ikhlaq et al. [25] studied the role of adsorption in the ozonation of ibuprofen, acetic acid, cumene, 1,2-dichlorobenzene and 1,2,4-trichlorobenzene by using commercial $\gamma\text{-Al}_2\text{O}_3$. Catalytic ozonation was carried out in a fixed-bed semi-batch reactor by using a catalyst concentration of 10.2 g/L and an ozone dose of 12–61 mg/L·h ($Q_{\text{gas}} = 0.006\text{--}0.03 \text{ L/h}$, $V_{\text{liq}} = 0.49 \text{ L}$ and solid : TOC = 593–5950). The reaction tests (single ozonation, adsorption of the main pollutant and catalytic ozonation) were monitored in terms of the main pollutant removal. The authors hypothesized two possible ozonation mechanisms: 1) the alumina promotes ozone decomposition leading to the production of $\bullet\text{OH}$ and other reactive species and surface OH-

groups may or may not be involved as the active sites; 2) the hydroxyl radicals may be formed in bulk solution reacting with the dissolved pollutants or with the adsorbed organics at the catalyst surface.

From all this survey, it can be clearly seen that adsorption plays a major role in the ozonation with alumina. For some authors, the adsorption of organics has favorable influence, whereas for others it is detrimental for catalytic activity. Some studies registered ozone decomposition, while others reported that alumina is inert towards O_3 ; therefore, the mechanism of ROS production is still not clear. In general, the higher oxidation performance with alumina was attributed to the interaction between ozone/organics with OH-groups on the alumina surface. Additionally, it seems that crystalline structure, thermal history and surface properties such as acidity, porosity and PZC are decisive features of the catalytic materials. Therefore, it should be noted that most studies performed the oxidation tests by using commercial alumina and only little characterization of them was informed.

From the results obtained in this research ($[solid] \approx 1 \text{ g/L}$, ozone dose = $420 \text{ mg/L}\cdot\text{h}$, $O_3 = 10 \text{ mg/L}$, $Q_{gas} = 42 \text{ L/h}$, $V_{liq} = 1 \text{ L}$ and a mass ratio of solid : TOC = 103), the catalysts based on ordered mesoporous alumina are capable of decomposing ozone, accordingly to the reported TOD values and ozone decomposition experiments. As was previously commented, it is possible to disregard the presence of alkaline residues from the proposed synthesis procedure. From the specific adsorption tests presented in section 2.2.6, it is possible to confirm that the high TOC removal with ordered mesoporous alumina is mainly due to the adsorption of polar oxidized by-products. The development of a heterogeneous catalytic mechanism cannot be excluded since the materials are able to decompose ozone; however, the total effect of ozonation with MA was alike the combined effect of adsorption on MA and single ozonation performed at the same pH, which indicates that under the selected operating conditions, the catalytic contribution is low. According to the surface coordination model, the registered TOC removal can be interpreted in terms of ligand exchange and electrostatic interactions between the OH-groups on the hydrous surface and polar by-products, probably carboxylates, since carboxylic acids are widely known as the main oxidation by-products of organic molecules. The results further indicate that, under the selected operating conditions, ferric species did not significantly contribute to the catalytic activity despite its higher surface acidity, in relation with bare MA.

To deepen the understanding on the role of solid materials in ozonation processes, further work is under way in order to investigate the nature of ROS, the nature of surface active sites and the catalytic effect in the presence of different model organic molecules.

2.2.9. Influence of water matrix

The oxidation rate of emerging pollutants may be largely affected by the nature of the water matrix. The constituent species of real water matrices can be organic (e.g. dissolved organic matter) or inorganic such as phosphate, sulphate, nitrite, chloride, carbonate and bicarbonate. These substances can impact on the performance of oxidation treatments having neutral, inhibitory or promoting effects [80]. In order to emulate a more real wastewater matrix, it was assessed the influence of different liquid matrices such as bottled water and a secondary effluent from a municipal wastewater treatment plant. These water matrices were spiked with SMX an ozonation experiments were performed as described before. Figure 11 shows the ozonation results; for the sake of comparison, ozonation with MA performed in ultrapure water was also graphed.

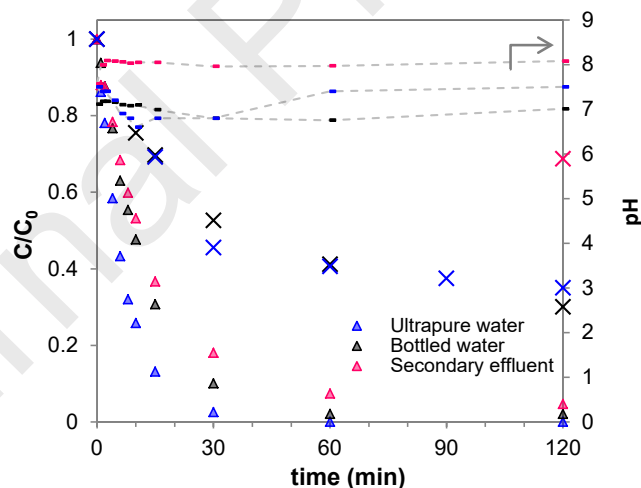


Figure 11. Ozonation with MA reported as dimensionless values of UVA₂₅₄ (△) and TOC (×). Effect of water matrix. (Operating conditions: $Q_{\text{gas}} = 42$ L/h NTP, $[O_3]_{\text{gas}} = 10$ mg/L NTP, $[SMX] = 20$ mg/L, $T = 22$ °C).

It can be seen from Fig. 11 that the removal rate of aromatics was delayed in the ozonation tests carried out with bottled water and the real wastewater in comparison with the results obtained by using ultrapure water.

For real water matrices, the ozone decomposition can be considerably lowered by the presence of radical scavengers such as (bi)carbonates, nitrite, chloride, among others [2]. However, the ions present in bottled water did not affect the elimination of organic matter reaching a final TOC removal of 70% (corresponding TOD = 308 mg/L), meaning that the constituents of bottled water did not interact with the surface sites of MA. Conversely, the performance of MA was significantly affected in the assays with the secondary effluent spiked with SMX, achieving a TOC removal of 31% (corresponding TOD = 301 mg/L). In this case, the constituents of the real effluent compete for the binding surface sites of mesoporous alumina. Hence, as adsorption plays a major role in the ozonation with alumina, the process will be more effective when treating cleaner water matrices such as wastewater from pharmaceutical industries.

3. Conclusions

Ordered mesoporous alumina (MA) and Fe-doped MA were synthesized by a facile sol-gel route at room temperature. The materials revealed an organized pore structure with cylindrical channels of c.a. 10 nm and amorphous walls, displaying significant microstructural differences in relation with commercial alumina. The materials were tested as potential catalysts/adsorbents in the ozonation of a pharmaceutical compound, sulfamethoxazole (SMX). In these combined experiments, the SMX was mainly oxidized through direct ozone reactions while the remaining TOC was removed in the presence of MA materials, reaching a remarkable TOC removal up to 86% (without pH adjustment, $pH_0 = 4.8$).

The reaction mechanism was studied taking into account the adsorption of by-products, pH effect and the role of Fe. According to the results obtained, MA materials behaved as strong adsorbents with scarce catalytic effect. The Fe leaching was negligible in all cases and the ferric species supported on alumina did not show significant catalytic activity under the conditions tested. Hence, the removal of SMX and its oxidation intermediates resulted mainly from the sum of direct ozone reactions and adsorption of by-products onto the alumina surface, even at neutral pH.

In order to give a more realistic approach, a real secondary effluent was spiked with the antibiotic. The aromatics abatement was slower to that observed in the ultrapure water matrix and the final TOC removal diminished to 31% due to presence of inhibitory substances, which blocked the surface sorption sites. In

addition, the matrix effect was evaluated using bottled water, and in this case, no inhibition was observed. Then, the process and materials proposed in this work would be more appropriate in matrices with a lower content of interferers.

In summary, under the chosen operating conditions, ordered mesoporous alumina behaved as strong adsorbent. Despite the ability to decompose ozone, the registered catalytic contribution was low. Hereafter, single ozonation might be employed to increase the polarity of oxidized compounds, which are more feasibly adsorbed onto the alumina surface. The pre-oxidation of organic matter might be a convenient strategy to improve the removal of pharmaceutical compounds by using good adsorbents such as mesoporous alumina. Furthermore, the spent material can be regenerated by direct ozonation in gas phase.

Acknowledgments

This work was financially supported by the Spanish Ministry of Economy and Competitiveness (project CTQ2014-52607-R), the Agency for Management of University and Research Grants of the Government of Catalonia (project 2014SGR245). The Argentinian authors wish to thank financial support from CONICET (PIP 112-201701-00844CO), UNMdP and ANPCyT (PICT-2017-3729).

References

- [1] J. Rivera-Utrilla, M. Sánchez-Polo, M.Á. Ferro-García, G. Prados-Joya, R. Ocampo-Pérez, Pharmaceuticals as emerging contaminants and their removal from water. A review, *Chemosphere*. 93 (2013) 1268–1287. <https://doi.org/10.1016/j.chemosphere.2013.07.059>.
- [2] J. Gomes, R. Costa, R.M. Quinta-Ferreira, R.C. Martins, Application of ozonation for pharmaceuticals and personal care products removal from water, *Sci. Total Environ*. 586 (2017) 265–283. <https://doi.org/10.1016/j.scitotenv.2017.01.216>.
- [3] J. Akhtar, N.S. Amin, A. Aris, Combined adsorption and catalytic ozonation for removal of sulfamethoxazole using Fe₂O₃/CeO₂ loaded activated carbon, *Chem. Eng. J.* 170 (2011) 136–144. <https://doi.org/10.1016/j.cej.2011.03.043>.

- [4] L. Rizzo, S. Malato, D. Antakyali, V.G. Beretsou, M.B. Đolić, W. Gernjak, E. Heath, I. Ivancev-Tumbas, P. Karaolia, A.R. Lado Ribeiro, G. Mascolo, C.S. McArdell, H. Schaar, A.M.T. Silva, D. Fatta-Kassinos, Consolidated vs new advanced treatment methods for the removal of contaminants of emerging concern from urban wastewater, *Sci. Total Environ.* 655 (2019) 986–1008. <https://doi.org/10.1016/j.scitotenv.2018.11.265>.
- [5] J. Wang, R. Zhuan, Degradation of antibiotics by advanced oxidation processes: An overview, *Sci. Total Environ.* 701 (2020) 135023. <https://doi.org/10.1016/j.scitotenv.2019.135023>.
- [6] G. Gao, J. Kang, J. Shen, Z. Chen, W. Chu, Heterogeneous Catalytic Ozonation of Sulfamethoxazole in Aqueous Solution over Composite Iron–Manganese Silicate Oxide, *Ozone Sci. Eng.* 39 (2017) 24–32. <https://doi.org/10.1080/01919512.2016.1237280>.
- [7] F.J. Beltrán, A. Rey, Free Radical and Direct Ozone Reaction Competition to Remove Priority and Pharmaceutical Water Contaminants with Single and Hydrogen Peroxide Ozonation Systems, *Ozone Sci. Eng.* 40 (2018) 251–265. <https://doi.org/10.1080/01919512.2018.1431521>.
- [8] A.S.C. Chen, V.L. Snoeyink, J. Mallevialle, F. Fiessinger, Activated Alumina for Removing Dissolved Organic Compounds, *J. Am. Water Works Assoc.* 81 (1989) 53–60.
- [9] J. Nawrocki, B. Kasprzyk-Hordern, The efficiency and mechanisms of catalytic ozonation, *Appl. Catal. B Environ.* 99 (2010) 27–42. <https://doi.org/10.1016/j.apcatb.2010.06.033>.
- [10] J. Wang, Z. Bai, Fe-based catalysts for heterogeneous catalytic ozonation of emerging contaminants in water and wastewater, *Chem. Eng. J.* 312 (2017) 79–98. <https://doi.org/10.1016/j.cej.2016.11.118>.
- [11] J. Akhtar, N.A.S. Amin, K. Shahzad, A review on removal of pharmaceuticals from water by adsorption, *Desalination Water Treat.* 57 (2016) 12842–12860. <https://doi.org/10.1080/19443994.2015.1051121>.
- [12] B. Kasprzyk-Hordern, M. Ziółek, J. Nawrocki, Catalytic ozonation and methods of enhancing molecular ozone reactions in water treatment, *Appl. Catal. B Environ.* 46 (2003) 639–669. [https://doi.org/10.1016/S0926-3373\(03\)00326-6](https://doi.org/10.1016/S0926-3373(03)00326-6).

- [13] M. Trueba, S.P. Trasatti, γ -Alumina as a Support for Catalysts: A Review of Fundamental Aspects, *Eur. J. Inorg. Chem.* 2005 (2005) 3393–3403. <https://doi.org/10.1002/ejic.200500348>.
- [14] B. Kasprzyk-Hordern, Chemistry of alumina, reactions in aqueous solution and its application in water treatment, *Adv. Colloid Interface Sci.* 110 (2004) 19–48. <https://doi.org/10.1016/j.cis.2004.02.002>.
- [15] G. Busca, The surface of transitional aluminas: A critical review, *Catal. Today.* 226 (2014) 2–13. <https://doi.org/10.1016/j.cattod.2013.08.003>.
- [16] C. Márquez-Alvarez, N. Žilková, J. Pérez-Pariente, J. Čejka, Synthesis, Characterization and Catalytic Applications of Organized Mesoporous Aluminas, *Catal. Rev.* 50 (2008) 222–286. <https://doi.org/10.1080/01614940701804042>.
- [17] Q. Yuan, A.-X. Yin, C. Luo, L.-D. Sun, Y.-W. Zhang, W.-T. Duan, H.-C. Liu, C.-H. Yan, Facile Synthesis for Ordered Mesoporous γ -Aluminas with High Thermal Stability, *J. Am. Chem. Soc.* 130 (2008) 3465–3472. <https://doi.org/10.1021/ja0764308>.
- [18] S.M. Morris, P.F. Fulvio, M. Jaroniec, Ordered Mesoporous Alumina-Supported Metal Oxides, *J. Am. Chem. Soc.* 130 (2008) 15210–15216. <https://doi.org/10.1021/ja806429q>.
- [19] C. di Luca, P. Massa, J.M. Grau, S.G. Marchetti, R. Fenoglio, P. Haure, Highly dispersed Fe³⁺-Al₂O₃ for the Fenton-like oxidation of phenol in a continuous up-flow fixed bed reactor. Enhancing catalyst stability through operating conditions, *Appl. Catal. B Environ.* 237 (2018) 1110–1123. <https://doi.org/10.1016/j.apcatb.2018.05.032>.
- [20] W. Cai, J. Yu, C. Anand, A. Vinu, M. Jaroniec, Facile Synthesis of Ordered Mesoporous Alumina and Alumina-Supported Metal Oxides with Tailored Adsorption and Framework Properties, *Chem. Mater.* 23 (2011) 1147–1157. <https://doi.org/10.1021/cm102512v>.
- [21] J. Nawrocki, Catalytic ozonation in water: Controversies and questions. Discussion paper, *Appl. Catal. B Environ.* 142–143 (2013) 465–471. <https://doi.org/10.1016/j.apcatb.2013.05.061>.
- [22] F.J. Beltrán, P. Pocostales, P.M. Álvarez, F. López-Piñeiro, Catalysts to improve the abatement of sulfamethoxazole and the resulting organic carbon in water during ozonation, *Appl. Catal. B Environ.* 92 (2009) 262–270. <https://doi.org/10.1016/j.apcatb.2009.08.001>.

- [23] M. Ernst, F. Lurot, J.-C. Schrotter, Catalytic ozonation of refractory organic model compounds in aqueous solution by aluminum oxide, *Appl. Catal. B Environ.* 47 (2004) 15–25.
[https://doi.org/10.1016/S0926-3373\(03\)00290-X](https://doi.org/10.1016/S0926-3373(03)00290-X).
- [24] G. Gao, J. Kang, J. Shen, Z. Chen, W. Chu, Catalytic ozonation of sulfamethoxazole by composite iron-manganese silicate oxide: cooperation mechanism between adsorption and catalytic reaction, *Environ. Sci. Pollut. Res.* 23 (2016) 21360–21368.
<https://doi.org/10.1007/s11356-016-7376-8>.
- [25] A. Ikhlaq, D.R. Brown, B. Kasprzyk-Hordern, Catalytic ozonation for the removal of organic contaminants in water on alumina, *Appl. Catal. B Environ.* 165 (2015) 408–418.
<https://doi.org/10.1016/j.apcatb.2014.10.010>.
- [26] R. Keykavoos, R. Mankidy, H. Ma, P. Jones, J. Soltan, Mineralization of bisphenol A by catalytic ozonation over alumina, *Sep. Purif. Technol.* 107 (2013) 310–317.
<https://doi.org/10.1016/j.seppur.2013.01.050>.
- [27] J. Vittenet, W. Aboussaoud, J. Mendret, J.-S. Pic, H. Debellefontaine, N. Lesage, K. Faucher, M.-H. Manero, F. Thibault-Starzyk, H. Leclerc, A. Galarneau, S. Brosillon, Catalytic ozonation with $\gamma\text{-Al}_2\text{O}_3$ to enhance the degradation of refractory organics in water, *Appl. Catal. Gen.* 504 (2015) 519–532. <https://doi.org/10.1016/j.apcata.2014.10.037>.
- [28] J. Nawrocki, L. Fijołek, Effect of aluminium oxide contaminants on the process of ozone decomposition in water, *Appl. Catal. B Environ.* 142–143 (2013) 533–537.
<https://doi.org/10.1016/j.apcatb.2013.05.069>.
- [29] W. Yang, B. Vogler, Y. Lei, T. Wu, Metallic ion leaching from heterogeneous catalysts: an overlooked effect in the study of catalytic ozonation processes, *Env. Sci Water Res Technol.* 3 (2017) 1143–1151. <https://doi.org/10.1039/C7EW00273D>.
- [30] N. Inchaurreondo, C. di Luca, G. Žerjav, J.M. Grau, A. Pintar, P. Haure, Catalytic ozonation of an azo-dye using a natural aluminosilicate, *Catal. Today.* (2019).
<https://doi.org/10.1016/j.cattod.2019.12.019>.

- [31] N. Inchaurredo, C. di Luca, F. Mori, A. Pintar, G. Žerjav, M. Valiente, C. Palet, Synthesis and adsorption behavior of mesoporous alumina and Fe-doped alumina for the removal of dominant arsenic species in contaminated waters, *J. Environ. Chem. Eng.* 7 (2019) 102901. <https://doi.org/10.1016/j.jece.2019.102901>.
- [32] N.K. Vel Leitner, B. Delouane, B. Legube, F. Luck, Effects Of Catalysts During Ozonation Of Salicylic Acid, Peptides And Humic Substances In Aqueous Solution, *Ozone Sci. Eng.* 21 (1999) 261–276. <https://doi.org/10.1080/01919519908547240>.
- [33] F.J. Beltrán, F.J. Rivas, R. Montero-de-Espinosa, Iron type catalysts for the ozonation of oxalic acid in water, *Water Res.* 39 (2005) 3553–3564. <https://doi.org/10.1016/j.watres.2005.06.018>.
- [34] B. Kasprzyk-Hordern, U. Raczky-Stanisławiak, J. Świetlik, J. Nawrocki, Catalytic ozonation of natural organic matter on alumina, *Appl. Catal. B Environ.* 62 (2006) 345–358. <https://doi.org/10.1016/j.apcatb.2005.09.002>.
- [35] Z. Yunrui, Z. Wanpeng, L. Fudong, W. Jianbing, Y. Shaoxia, Catalytic activity of Ru/Al₂O₃ for ozonation of dimethyl phthalate in aqueous solution, *Chemosphere.* 66 (2007) 145–150. <https://doi.org/10.1016/j.chemosphere.2006.04.087>.
- [36] F. Qi, B. Xu, Z. Chen, L. Feng, L. Zhang, D. Sun, Catalytic ozonation of 2-isopropyl-3-methoxypyrazine in water by γ -AlOOH and γ -Al₂O₃: Comparison of removal efficiency and mechanism, *Chem. Eng. J.* 219 (2013) 527–536. <https://doi.org/10.1016/j.cej.2013.01.035>.
- [37] M. Trapido, Y. Veressinina, R. Munter, J. Kallas, Catalytic Ozonation of m-Dinitrobenzene, *Ozone Sci. Eng.* 27 (2005) 359–363. <https://doi.org/10.1080/01919510500250630>.
- [38] A. Ziylan-Yavaş, N.H. Ince, Catalytic ozonation of paracetamol using commercial and Pt-supported nanocomposites of Al₂O₃: The impact of ultrasound, *Ultrason. Sonochem.* 40 (2018) 175–182. <https://doi.org/10.1016/j.ultsonch.2017.02.017>.
- [39] P. Pocostales, P. Álvarez, F.J. Beltrán, Catalytic ozonation promoted by alumina-based catalysts for the removal of some pharmaceutical compounds from water, *Chem. Eng. J.* 168 (2011) 1289–1295. <https://doi.org/10.1016/j.cej.2011.02.042>.

- [40] L. Chen, F. Qi, B. Xu, Z. Xu, J. Shen, K. Li, The efficiency and mechanism of γ -alumina catalytic ozonation of 2-methylisoborneol in drinking water, *Water Sci. Technol. Water Supply*. 6 (2006) 43–51. <https://doi.org/10.2166/ws.2006.726>.
- [41] A. Ikhlaq, D.R. Brown, B. Kasprzyk-Hordern, Mechanisms of catalytic ozonation: An investigation into superoxide ion radical and hydrogen peroxide formation during catalytic ozonation on alumina and zeolites in water, *Appl. Catal. B Environ.* 129 (2013) 437–449. <https://doi.org/10.1016/j.apcatb.2012.09.038>.
- [42] C.H. Ni, J.N. Chen, Heterogeneous catalytic ozonation of 2-chlorophenol aqueous solution with alumina as a catalyst, *Water Sci Technol.* 43 (2001) 213–20. <https://doi.org/PMID:11380182>.
- [43] F. Qi, B. Xu, Z. Chen, J. Ma, D. Sun, L. Zhang, Influence of aluminum oxides surface properties on catalyzed ozonation of 2,4,6-trichloroanisole, *Sep. Purif. Technol.* 66 (2009) 405–410. <https://doi.org/10.1016/j.seppur.2009.01.013>.
- [44] L. Yang, C. Hu, Y. Nie, J. Qu, Surface acidity and reactivity of β -FeOOH/Al₂O₃ for pharmaceuticals degradation with ozone: In situ ATR-FTIR studies, *Appl. Catal. B Environ.* 97 (2010) 340–346. <https://doi.org/10.1016/j.apcatb.2010.04.014>.
- [45] Z.S. Ncanana, V.S.R. Rajasekhar Pullabhotla, Oxidative degradation of m-cresol using ozone in the presence of pure γ -Al₂O₃, SiO₂ and V₂O₅ catalysts, *J. Environ. Chem. Eng.* 7 (2019) 103072. <https://doi.org/10.1016/j.jece.2019.103072>.
- [46] D. Polat, İ. Balcı, T.A. Özbelge, Catalytic ozonation of an industrial textile wastewater in a heterogeneous continuous reactor, *J. Environ. Chem. Eng.* 3 (2015) 1860–1871. <https://doi.org/10.1016/j.jece.2015.04.020>.
- [47] C. Chen, Y. Chen, B. Yoza, Y. Du, Y. Wang, Q. Li, L. Yi, S. Guo, Q. Wang, Comparison of Efficiencies and Mechanisms of Catalytic Ozonation of Recalcitrant Petroleum Refinery Wastewater by Ce, Mg, and Ce-Mg Oxides Loaded Al₂O₃, Catalysts. 7 (2017) 72. <https://doi.org/10.3390/catal7030072>.
- [48] A. Aghaeinejad-Meybodi, A. Ebadi, S. Shafiei, A. Khataee, A.D. Kiadehi, Degradation of Fluoxetine using catalytic ozonation in aqueous media in the presence of nano- γ -alumina

- catalyst: Experimental, modeling and optimization study, *Sep. Purif. Technol.* 211 (2019) 551–563. <https://doi.org/10.1016/j.seppur.2018.10.020>.
- [49] A.K.H. Al jibouri, J. Wu, S.R. Upreti, Heterogeneous catalytic ozonation of naphthenic acids in water, *Can. J. Chem. Eng.* 97 (2019) 67–73. <https://doi.org/10.1002/cjce.23209>.
- [50] J.S. Salla, N. Padoin, S.M. Amorim, G. Li Puma, R.F.P.M. Moreira, Humic acids adsorption and decomposition on Mn₂O₃ and α -Al₂O₃ nanoparticles in aqueous suspensions in the presence of ozone, *J. Environ. Chem. Eng.* 8 (2020) 102780. <https://doi.org/10.1016/j.jece.2018.11.025>.
- [51] Y. He, H. Zhang, J. Li, Y. Zhang, B. Lai, Z. Pan, Treatment of Landfill Leachate Reverse Osmosis Concentrate from by Catalytic Ozonation with γ -Al₂O₃, *Environ. Eng. Sci.* 35 (2018) 501–511. <https://doi.org/10.1089/ees.2017.0188>.
- [52] A.G. Gonçalves, J.J.M. Órfão, M.F.R. Pereira, Catalytic ozonation of sulphamethoxazole in the presence of carbon materials: Catalytic performance and reaction pathways, *J. Hazard. Mater.* 239–240 (2012) 167–174. <https://doi.org/10.1016/j.jhazmat.2012.08.057>.
- [53] A.G. Gonçalves, J.J.M. Órfão, M.F.R. Pereira, Ceria dispersed on carbon materials for the catalytic ozonation of sulfamethoxazole, *J. Environ. Chem. Eng.* 1 (2013) 260–269. <https://doi.org/10.1016/j.jece.2013.05.009>.
- [54] A.G. Gonçalves, J.J.M. Órfão, M.F.R. Pereira, Ozonation of sulfamethoxazole promoted by MWCNT, *Catal. Commun.* 35 (2013) 82–87. <https://doi.org/10.1016/j.catcom.2013.02.012>.
- [55] D. Shahidi, A. Moheb, R. Abbas, S. Larouk, R. Roy, A. Azzouz, Total mineralization of sulfamethoxazole and aromatic pollutants through Fe²⁺-montmorillonite catalyzed ozonation, *J. Hazard. Mater.* 298 (2015) 338–350. <https://doi.org/10.1016/j.jhazmat.2015.05.029>.
- [56] R. Yin, W. Guo, X. Zhou, H. Zheng, J. Du, Q. Wu, J. Chang, N. Ren, Enhanced sulfamethoxazole ozonation by noble metal-free catalysis based on magnetic Fe₃O₄ nanoparticles: catalytic performance and degradation mechanism, *RSC Adv.* 6 (2016) 19265–19270. <https://doi.org/10.1039/C5RA25994K>.

- [57] R. Yin, W. Guo, J. Du, X. Zhou, H. Zheng, Q. Wu, J. Chang, N. Ren, Heteroatoms doped graphene for catalytic ozonation of sulfamethoxazole by metal-free catalysis: Performances and mechanisms, *Chem. Eng. J.* 317 (2017) 632–639. <https://doi.org/10.1016/j.cej.2017.01.038>.
- [58] J. Bing, C. Hu, L. Zhang, Enhanced mineralization of pharmaceuticals by surface oxidation over mesoporous γ -Ti-Al₂O₃ suspension with ozone, *Appl. Catal. B Environ.* 202 (2017) 118–126. <https://doi.org/10.1016/j.apcatb.2016.09.019>.
- [59] R.C. Martins, M. Cardoso, R.F. Dantas, C. Sans, S. Esplugas, R.M. Quinta-Ferreira, Catalytic studies for the abatement of emerging contaminants by ozonation: Catalytic studies on abatement of emerging contaminants by ozonation, *J. Chem. Technol. Biotechnol.* 90 (2015) 1611–1618. <https://doi.org/10.1002/jctb.4711>.
- [60] S.M. Morris, P.F. Fulvio, M. Jaroniec, Ordered Mesoporous Alumina-Supported Metal Oxides, *J. Am. Chem. Soc.* 130 (2008) 15210–15216. <https://doi.org/10.1021/ja806429q>.
- [61] T. Preočanin, N. Kallay, Application of »Mass Titration« to Determination of Surface Charge of Metal Oxides, *CROATICA CHEMICA ACTA.* 71 (1998) 1117–1125.
- [62] M. Marce, B. Domenjoud, S. Esplugas, S. Baig, Ozonation treatment of urban primary and biotreated wastewaters: Impacts and modeling, *Chem. Eng. J.* 283 (2016) 768–777. <https://doi.org/10.1016/j.cej.2015.07.073>.
- [63] M.L. Wilde, S. Montipó, A.F. Martins, Degradation of β -blockers in hospital wastewater by means of ozonation and Fe²⁺/ozonation, *Water Res.* 48 (2014) 280–295. <https://doi.org/10.1016/j.watres.2013.09.039>.
- [64] H. Bader, J. Hoigné, Determination of ozone in water by the indigo method, *Water Res.* 15 (1981) 449–456. [https://doi.org/10.1016/0043-1354\(81\)90054-3](https://doi.org/10.1016/0043-1354(81)90054-3).
- [65] M. Thommes, K. Kaneko, A.V. Neimark, J.P. Olivier, F. Rodriguez-Reinoso, J. Rouquerol, K.S.W. Sing, Physisorption of gases, with special reference to the evaluation of surface area and pore size distribution (IUPAC Technical Report), *Pure Appl. Chem.* 87 (2015) 1051–1069. <https://doi.org/10.1515/pac-2014-1117>.

- [66] M. Kosmulski, The pH-Dependent Surface Charging and the Points of Zero Charge, *J. Colloid Interface Sci.* 253 (2002) 77–87. <https://doi.org/10.1006/jcis.2002.8490>.
- [67] R.F. Dantas, S. Contreras, C. Sans, S. Esplugas, Sulfamethoxazole abatement by means of ozonation, *J. Hazard. Mater.* 150 (2008) 790–794. <https://doi.org/10.1016/j.jhazmat.2007.05.034>.
- [68] S. Gao, Z. Zhao, Y. Xu, J. Tian, H. Qi, W. Lin, F. Cui, Oxidation of sulfamethoxazole (SMX) by chlorine, ozone and permanganate—A comparative study, *J. Hazard. Mater.* 274 (2014) 258–269. <https://doi.org/10.1016/j.jhazmat.2014.04.024>.
- [69] F. Qi, B. Xu, Z. Chen, L. Zhang, P. Zhang, D. Sun, Mechanism investigation of catalyzed ozonation of 2-methylisoborneol in drinking water over aluminum (hydroxyl) oxides: Role of surface hydroxyl group, *Chem. Eng. J.* 165 (2010) 490–499. <https://doi.org/10.1016/j.cej.2010.09.047>.
- [70] A.G. Trovó, R.F.P. Nogueira, A. Agüera, A.R. Fernandez-Alba, C. Sirtori, S. Malato, Degradation of sulfamethoxazole in water by solar photo-Fenton. Chemical and toxicological evaluation, *Water Res.* 43 (2009) 3922–3931. <https://doi.org/10.1016/j.watres.2009.04.006>.
- [71] M. del M. Gómez-Ramos, M. Mezcua, A. Agüera, A.R. Fernández-Alba, S. Gonzalo, A. Rodríguez, R. Rosal, Chemical and toxicological evolution of the antibiotic sulfamethoxazole under ozone treatment in water solution, *J. Hazard. Mater.* (2011). <https://doi.org/10.1016/j.jhazmat.2011.04.072>.
- [72] A.G. Trovó, R.F.P. Nogueira, A. Agüera, C. Sirtori, A.R. Fernández-Alba, Photodegradation of sulfamethoxazole in various aqueous media: Persistence, toxicity and photoproducts assessment, *Chemosphere.* 77 (2009) 1292–1298. <https://doi.org/10.1016/j.chemosphere.2009.09.065>.
- [73] J. Sarasa, Study of the aromatic by-products formed from ozonation of anilines in aqueous solution, *Water Res.* 36 (2002) 3035–3044. [https://doi.org/10.1016/S0043-1354\(02\)00003-9](https://doi.org/10.1016/S0043-1354(02)00003-9).
- [74] M.N. Abellán, W. Gebhardt, H.Fr. Schröder, Detection and identification of degradation products of sulfamethoxazole by means of LC/MS and –MSn after ozone treatment, *Water Sci. Technol.* 58 (2008) 1803–1812. <https://doi.org/10.2166/wst.2008.539>.

- [75] F.J. Beltrán, A. Aguinaco, J.F. García-Araya, A. Oropesa, Ozone and photocatalytic processes to remove the antibiotic sulfamethoxazole from water, *Water Res.* 42 (2008) 3799–3808.
<https://doi.org/10.1016/j.watres.2008.07.019>.
- [76] H. Yan, W. Chen, G. Liao, X. Li, S. Ma, L. Li, Activity assessment of direct synthesized Fe-SBA-15 for catalytic ozonation of oxalic acid, *Sep. Purif. Technol.* 159 (2016) 1–6.
<https://doi.org/10.1016/j.seppur.2015.12.055>.
- [77] W. Chen, X. Li, Z. Pan, S. Ma, L. Li, Effective mineralization of Diclofenac by catalytic ozonation using Fe-MCM-41 catalyst, *Chem. Eng. J.* 304 (2016) 594–601.
<https://doi.org/10.1016/j.cej.2016.06.139>.
- [78] R. Huang, H. Yan, L. Li, D. Deng, Y. Shu, Q. Zhang, Catalytic activity of Fe/SBA-15 for ozonation of dimethyl phthalate in aqueous solution, *Appl. Catal. B Environ.* (2011).
<https://doi.org/10.1016/j.apcatb.2011.05.041>.
- [79] N. Al-Hayek, B. Legube, M. Doré, Ozonation catalytique (Fe III/Al₂O₃) Du phénol et de ses produits d'ozonation, *Environ. Technol. Lett.* 10 (1989) 415–426.
<https://doi.org/10.1080/09593338909384757>.
- [80] A.R. Lado Ribeiro, N.F.F. Moreira, G. Li Puma, A.M.T. Silva, Impact of water matrix on the removal of micropollutants by advanced oxidation technologies, *Chem. Eng. J.* 363 (2019) 155–173. <https://doi.org/10.1016/j.cej.2019.01.080>.

Figure captions

Figure 1. Scheme of the ozonation installation: 1) ozone generator, 2) inlet O₃ analyzer, 3) outlet O₃ analyzer and 4) stirred-tank reactor.

Figure 2. TEM images of synthesized mesoporous aluminas (MA) and commercial γ -Al₂O₃ (CA).

Figure 3. N₂ Physisorption results: isotherms at -196 °C (A) and pore size distribution (B).

Figure 4. Ozonation of sulfamethoxazole reported as dimensionless values of SMX, UVA₂₅₄ and TOC.

Effect of pH: A) SMX decomposition; B) pH profiles and C) TOC removal (×) and UVA₂₅₄ (Δ).

(Operating conditions: Q_{gas} = 42 L/h NTP, [O₃]_{gas} = 10 mg/L NTP, [SMX] = 20 mg/L, T = 22 °C).

Figure 5. Ozone profiles for single ozonation and ozonation with MA and MA-5Fe. (Operating conditions: $Q_{\text{gas}} = 42$ L/h NTP, $[\text{O}_3]_{\text{gas}} = 10$ mg/L NTP, $[\text{SMX}] = 20$ mg/L, $T = 22$ °C, $\text{pH}_0 = 4.8$).

Figure 6. Ozonation with MA and MA-5Fe. (Operating conditions: $Q_{\text{gas}} = 42$ L/h NTP, $[\text{O}_3]_{\text{gas}} = 10$ mg/L NTP, $[\text{SMX}] = 20$ mg/L, $T = 22$ °C, $[\text{solid}] \approx 1$ g/L).

Figure 7. Evolution of dimensionless remaining ozone concentration with time during its decomposition in different water matrices (UW: ultrapure water, SSO120: supernatant of single ozonation collected at 120 min and SCO120: supernatant of catalytic ozonation collected at 120 min) in the absence and presence of MA and MA-5Fe (operating conditions: $V = 500$ mL, $[\text{O}_3]_{\text{liq}} = 1.5\text{--}2$ mg/L, $[\text{solid}] = 1$ g/L and $T = 22$ °C).

Figure 8. Ozonation with homogeneous Fe^{3+} reported as dimensionless values of SMX and TOC (operating conditions: $Q_{\text{gas}} = 42$ L/h NTP, $[\text{O}_3]_{\text{gas}} = 10$ mg/L NTP, $[\text{SMX}] = 20$ mg/L, $T = 22$ °C, $[\text{Fe}^{3+}] = 10$ ppm).

Figure 9. Adsorption and catalytic ozonation of by-products. Experiment A: Adsorption of by-products on MA under oxygen flow; Experiment B: Catalytic ozonation of by-products with MA. Black columns represent tests without pH adjustment ($\text{pH}_0 = 3.6$) while the reds are at $\text{pH} = 7.5$ (operating conditions: $Q_{\text{gas}} = 42$ L/h NTP, $[\text{O}_3]_{\text{gas}} = 10$ mg/L NTP, $[\text{TOC}]_0 = 8.1$ mg/L, $T = 22$ °C, $t = 90$ min).

Figure 10. Single ozonation carried out during 5, 15, 30 and 60 min followed of adsorption of by-products with MA-5Fe (operating conditions: $Q_{\text{gas}} = 21$ L/h NTP, $V = 500$ mL, $[\text{O}_3]_{\text{gas}} = 10$ mg/L NTP, $[\text{SMX}] = 20$ mg/L, $T = 22$ °C, $\text{pH}_0 = 4.8$, $[\text{solid}] = 1$ g/L).

Figure 11. Ozonation with MA reported as dimensionless values of UVA_{254} (Δ) and TOC (\times). Effect of water matrix. (Operating conditions: $Q_{\text{gas}} = 42$ L/h NTP, $[\text{O}_3]_{\text{gas}} = 10$ mg/L NTP, $[\text{SMX}] = 20$ mg/L, $T = 22$ °C).

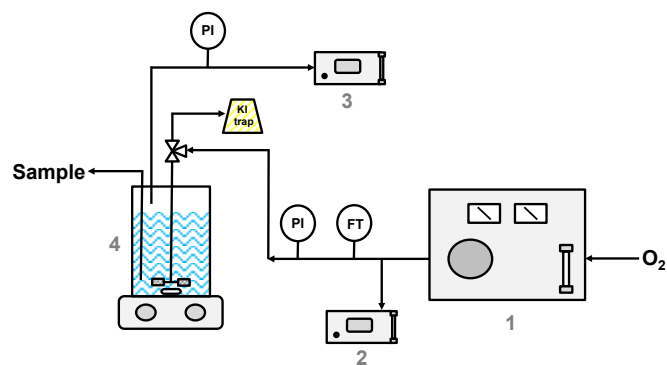


Figure 1. Scheme of the ozonation installation: 1) ozone generator, 2) inlet O₃ analyzer, 3) outlet O₃ analyzer and 4) stirred-tank reactor.

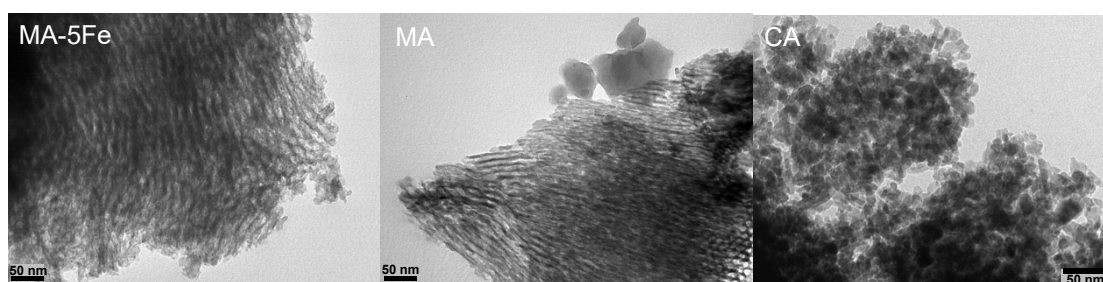


Figure 2. TEM images of synthesized mesoporous aluminas (MA) and commercial γ - Al_2O_3 (CA).

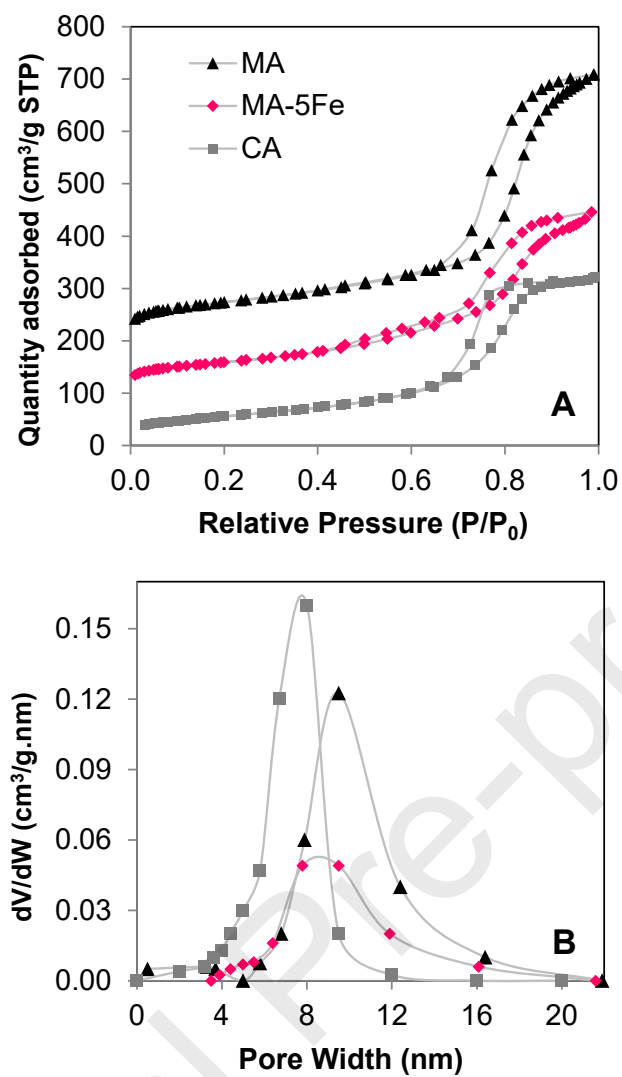


Figure 3. N₂ Physisorption results: isotherms at -196 °C (A) and pore size distribution (B).

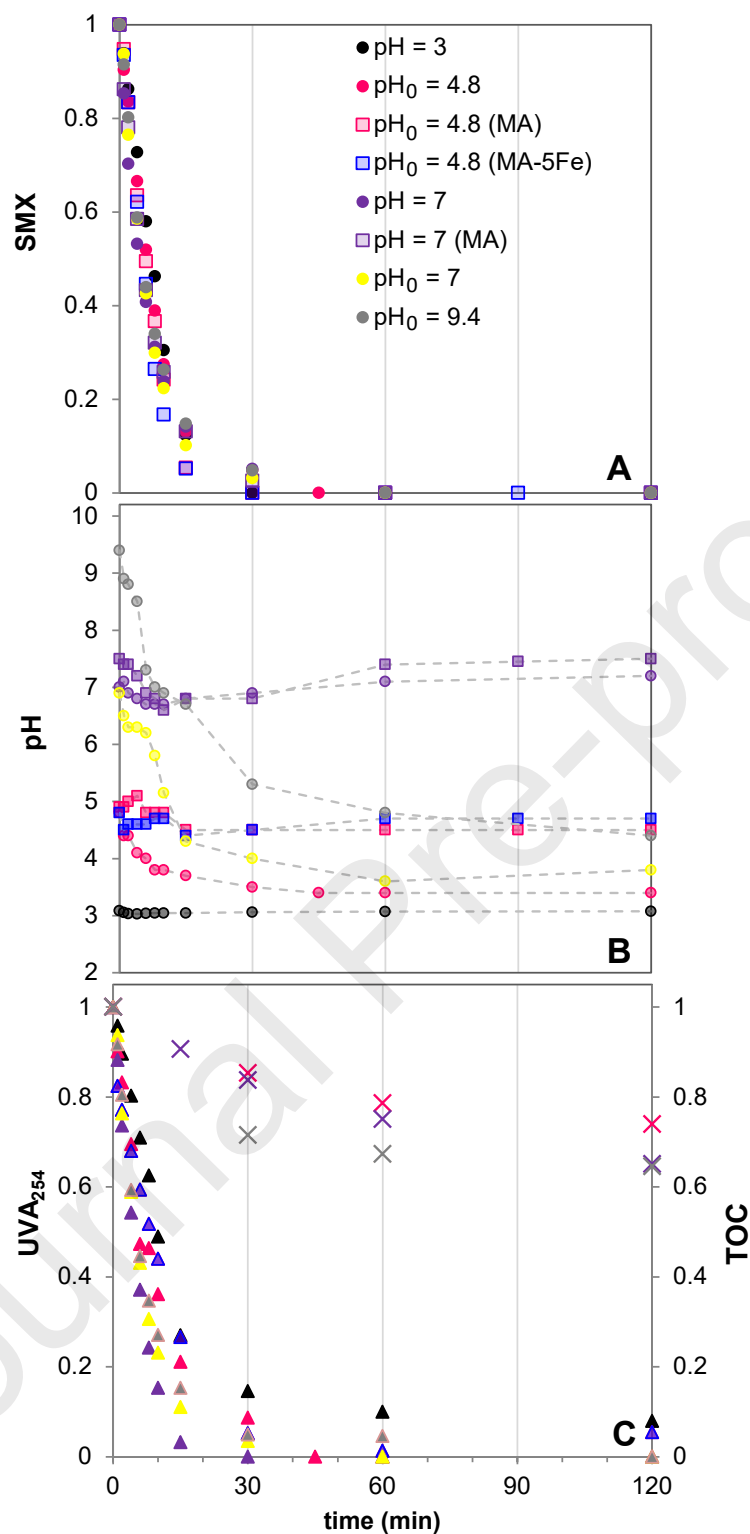


Figure 4. Ozonation of sulfamethoxazole reported as dimensionless values of SMX, UVA₂₅₄ and TOC.

Effect of pH: A) SMX decomposition; B) pH profiles and C) TOC removal (×) and UVA₂₅₄ (Δ).

(Operating conditions: $Q_{\text{gas}} = 42$ L/h NTP, $[\text{O}_3]_{\text{gas}} = 10$ mg/L NTP, $[\text{SMX}] = 20$ mg/L, $T = 22$ °C).

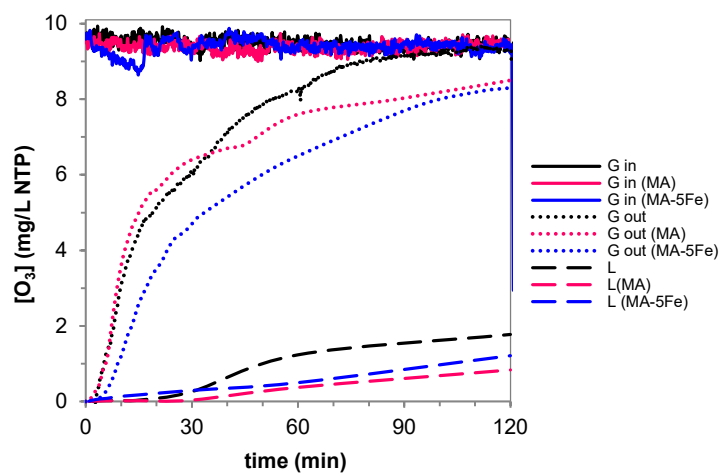


Figure 5. Ozone profiles for single ozonation and ozonation with MA and MA-5Fe. (Operating conditions: $Q_{\text{gas}} = 42$ L/h NTP, $[O_3]_{\text{gas}} = 10$ mg/L NTP, $[SMX] = 20$ mg/L, $T = 22$ °C, $pH_0 = 4.8$).

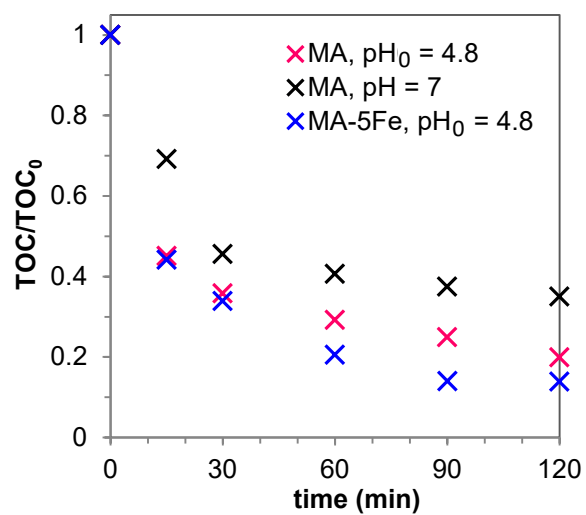


Figure 6. Ozonation with MA and MA-5Fe. (Operating conditions: $Q_{\text{gas}} = 42$ L/h NTP, $[O_3]_{\text{gas}} = 10$ mg/L NTP, $[SMX] = 20$ mg/L, $T = 22$ °C, $[\text{solid}] \approx 1$ g/L).

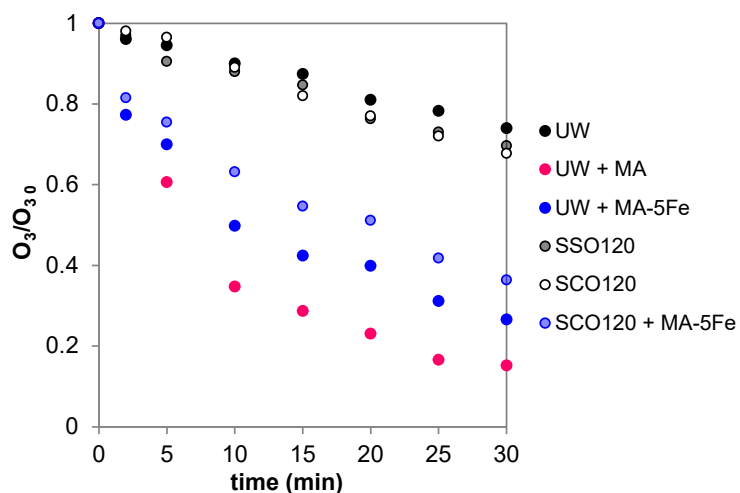


Figure 7. Evolution of dimensionless remaining ozone concentration with time during its decomposition in different water matrices (UW: ultrapure water, SSO120: supernatant of single ozonation collected at 120 min and SCO120: supernatant of catalytic ozonation collected at 120 min) in the absence and presence of MA and MA-5Fe (operating conditions: $V = 500$ mL, $[O_3]_{liq} = 1.5-2$ mg/L, $[solid] = 1$ g/L and $T = 22$ °C).

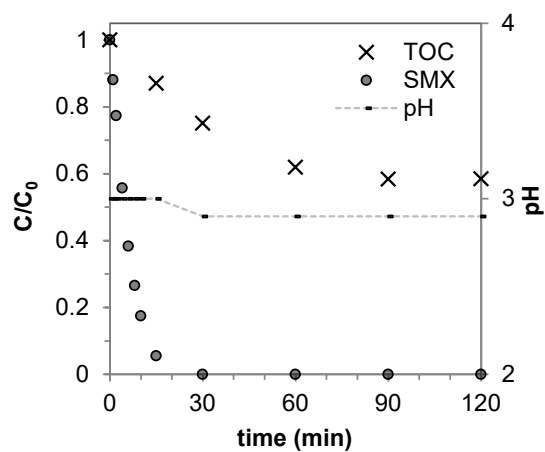


Figure 8. Ozonation with homogeneous Fe³⁺ reported as dimensionless values of SMX and TOC (operating conditions: $Q_{\text{gas}} = 42$ L/h NTP, $[O_3]_{\text{gas}} = 10$ mg/L NTP, $[SMX] = 20$ mg/L, $T = 22$ °C, $[Fe^{3+}] = 10$ ppm).

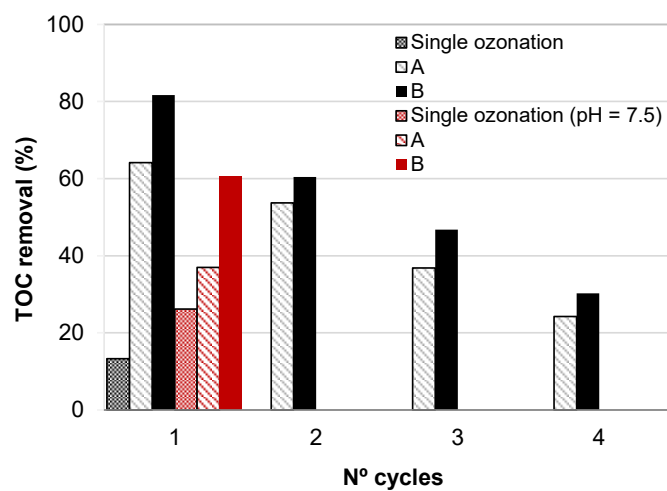


Figure 9. Adsorption and catalytic ozonation of by-products. Experiment A: Adsorption of by-products on MA under oxygen flow; Experiment B: Catalytic ozonation of by-products with MA. Black columns represent tests without pH adjustment ($\text{pH}_0 = 3.6$) while the reds are at $\text{pH} = 7.5$ (operating conditions: $Q_{\text{gas}} = 42 \text{ L/h NTP}$, $[\text{O}_3]_{\text{gas}} = 10 \text{ mg/L NTP}$, $[\text{TOC}]_0 = 8.1 \text{ mg/L}$, $T = 22 \text{ }^\circ\text{C}$, $t = 90 \text{ min}$).

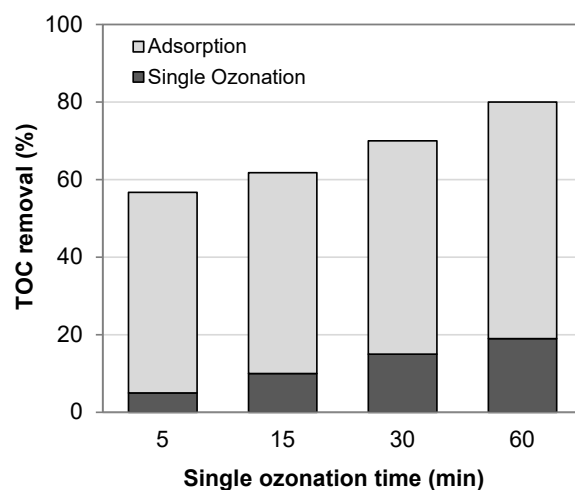


Figure 10. Single ozonation carried out during 5, 15, 30 and 60 min followed of adsorption of by-products with MA-5Fe (operating conditions: $Q_{\text{gas}} = 21$ L/h NTP, $V = 500$ mL, $[O_3]_{\text{gas}} = 10$ mg/L NTP, $[SMX] = 20$ mg/L, $T = 22$ °C, $pH_0 = 4.8$, $[\text{solid}] = 1$ g/L).

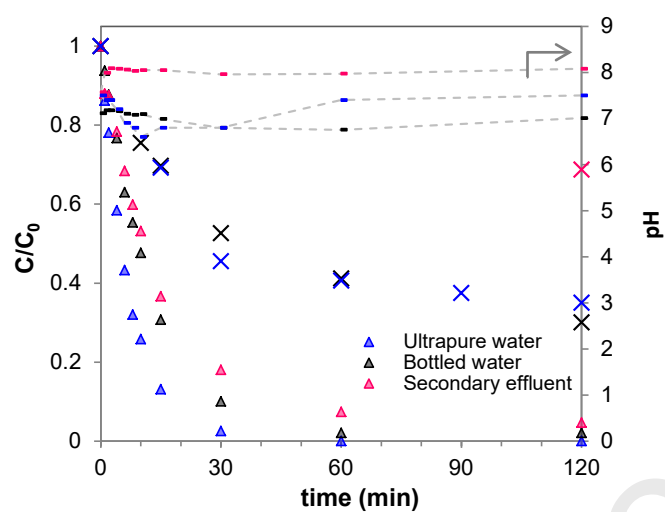


Figure 11. Ozonation with MA reported as dimensionless values of UVA₂₅₄ (Δ) and TOC (\times). Effect of water matrix. (Operating conditions: $Q_{\text{gas}} = 42$ L/h NTP, $[O_3]_{\text{gas}} = 10$ mg/L NTP, $[SMX] = 20$ mg/L, $T = 22$ °C).

Table captions

Table 1. Literature reports on alumina and Fe-doped alumina for the ozonation of organic pollutants.

Table 2. Literature reports on different solids in the ozonation of SMX.

Table 3. Characterization of the municipal secondary effluent used in this work.

Table 4. Summary of characterization outcomes.

Table 5. Accurate mass measurements found by LC-ESI(+)-TOF-MS spectra of protonated SMX and its degradation products.

Table 1. Literature reports on alumina and Fe-doped alumina for the ozonation of organic pollutants.

Pollutant	Solid material	Operating conditions	Removal results	Ref.
Humic substances TOC ₀ = 2.5-2.6 mg/L	Al ₂ O ₃	cat. 130 g/L, V _{liq} = 46 mL, room T, pH 7.2, O ₃ 2.5 mg/mg _{TOC} , t _{test} = 10 min, Slurry Batch reactor	Ads. X _{TOC} = 44 % O ₃ X _{TOC} = 13.8 % O ₃ + cat. X _{TOC} = 47.2 %	[32]
Salicylic acid TOC ₀ = 3 mg/L	Al ₂ O ₃	cat. 130 g/L, V _{liq} = 46 mL, room T, pH 7.2, O ₃ 2.5 mg/mg _{TOC} , t _{test} = 10 min, Slurry Batch reactor	Ads. X _{TOC} = 51.7 % O ₃ X _{TOC} = 12.7 % O ₃ + cat. X _{TOC} = 52.3 %	[32]
Peptide TOC ₀ = 2.5-2.6 mg/L	Al ₂ O ₃	cat. 130 g/L, V _{liq} = 46 mL, room T, pH 7.2, O ₃ 2.5 mg/mg _{TOC} , t _{test} = 10 min, Slurry Batch reactor	Ads. X _{TOC} = 0 % O ₃ X _{TOC} = 46 % O ₃ + cat. X _{TOC} = 15.4 %	[32]
Oxalic acid 0.008 mol/L	γ-Al ₂ O ₃	cat. 1.25 g/L, V _{liq} = 800 mL, 20°C, pH 2.5, Q _{gas} = 24 L/h, [O ₃] _{gas} = 30 mg/L, t _{test} = 3 h, SemiBatch reactor	O ₃ X _{oxalic} = 1-2 % O ₃ + cat. X _{oxalic} = 7 %	[33]
Oxalic acid 0.008 mol/L	γ-Al ₂ O ₃ -Fe ₂ O ₃	cat. 1.25 g/L, V _{liq} = 800 mL, 20 °C, pH 2.5, Q _{gas} = 24 L/h, [O ₃] _{gas} = 30 mg/L, t _{test} = 3 h, SemiBatch reactor	Ads. X _{oxalic} = 7 % O ₃ X _{oxalic} = 1-2 % O ₃ + cat. X _{oxalic} = 28 %	[33]
Bisphenol A 10 mg/L	γ-Al ₂ O ₃	cat. 1 g/L, 23 °C, pH ₀ 5, [O ₃] _{liq} = 4.5 mg/L, t _{test} = 1 h, Slurry Batch reactor	Ads. X _{TOC} = 87 % O ₃ X _{TOC} = 35 % O ₃ + cat. X _{TOC} = 90 %	[26]
2,4 dimethylphenol 50 mg/L	γ-Al ₂ O ₃	cat. 5 g/L, V _{liq} = 1.5 L, 25 °C, pH ₀ 4.5, Q _{gas} = 40 L/h, [O ₃] _{gas} = 2 g/Nm ³ , t _{test} = 300 min, Slurry SemiBatch reactor	O ₃ X _{TOC} = 14 % O ₃ + cat. X _{TOC} = 57 % Carboxylic acid adsorbed are difficult to accurately estimate	[27]
Tap water enriched with NOM DOC 28.7 mg/L	Al ₂ O ₃	cat. 30 g, V _{liq} = 0.4 L, 20 °C, pH 8, Q _{gas} = 19.5 mL/min, [O ₃] _{gas} = 0.4 mg/L min, t _{test} = 3 h, Fixed bed reactor semibatch	17 th Cycle O ₃ X _{TOC} = 31 % O ₃ + cat. X _{TOC} = 63 % Adsorption is the dominant process during the first cycles	[34]
Dimethyl phthalate (DMP) TOC ₀ = 4.03 mg/L	Al ₂ O ₃	cat. 10 g/L, 15 °C, pH ₀ 6.6, Q _{gas} = 0.4 L/min, [O ₃] _{dose} = 116 mg/h, t _{test} = 2 h, Slurry SemiBatch reactor	Ads. X _{DMP} = 5 % O ₃ X _{TOC} = 24 % O ₃ + cat. X _{TOC} = 56 % Byproducts adsorption could not be neglected	[35]
Ibuprofen 15 mg/L	γ-Al ₂ O ₃	cat. 5 g, V _{liq} = 0.49 L, 20 °C, pH 7.2, Q _{gas} = 0.5 mL/min, [O ₃] _{dose} = 0.5 mg/min, t _{test} = 30 min, Fixed bed SemiBatch reactor	Ads. X _{ibuprofen} = 13 % O ₃ X _{ibuprofen} = 40 % O ₃ + cat. X _{ibuprofen} = 83 %	[25]
Acetic acid 15 mg/L	γ-Al ₂ O ₃	cat. 5 g, V _{liq} = 0.49 L, 20 °C, pH 7.2, Q _{gas} = 0.5 mL/min, [O ₃] _{dose} = 0.5 mg/min, t _{test} = 30 min, Fixed bed SemiBatch reactor	Ads. X _{acetic} = 7 % O ₃ X _{acetic} = 6 % O ₃ + cat. X _{acetic} = 19 %	[25]
Cumene 19.1 mg/L	γ-Al ₂ O ₃	cat. 5 g, V _{liq} = 0.49 L, 20 °C, pH 7.2, Q _{gas} = 0.1 mL/min, [O ₃] _{dose} = 0.1 mg/min, t _{test} = 30 min, Fixed bed SemiBatch reactor	Ads. X _{cumene} = 5 %, O ₃ X _{cumene} = 60 %, O ₃ + cat. X _{cumene} = 58 %	[25]
1,2-dichlorobenzene 3.5 mg/L	γ-Al ₂ O ₃	cat. 5 g, V _{liq} = 0.49 L, 20 °C, pH 6.2, Q _{gas} = 0.1 mL/min, [O ₃] _{dose} = 0.1 mg/min, t _{test} = 30 min, Fixed bed SemiBatch reactor	Ads. X _{dichlorobenzene} = 7 % O ₃ X _{dichlorobenzene} = 61 % O ₃ + cat. X _{dichlorobenzene} = 45 %	[25]

2-isopropyl-3-methoxy pyrazine (IPMP) 38 µg/L	γ -Al ₂ O ₃	cat. 500 mg/L, pH 7.05, [O ₃] _{liq} = 0.5 mg/L, t _{test} = 10 min, Slurry Batch reactor	Ads. X _{IPMP} = 5 % O ₃ X _{IPMP} = 55 % O ₃ + cat. X _{IPMP} = 90 %	[36]
m-dinitrobenzene 1 mmol/L	Al ₂ O ₃	cat. 1 g/L, V _{liq} = 0.7 L, 20 °C, pH ₀ 3, Q _{gas} = 1 L/min, [O ₃] _{gas} = 12 mg/L, t _{test} = 2 h, Bubble Column SemiBatch reactor	O ₃ X _{COD} = 68 % O ₃ + cat. X _{COD} = 92 %	[37]
Paracetamol 35 µmol/L	Al ₂ O ₃	cat. 5 mg/L, V _{liq} = 0.7 L, pH 3, [O ₃] _{dose} = 3 mg/min, t _{test} = 1 h, Slurry SemiBatch reactor	O ₃ X _{TOC} = 4 %, O ₃ + cat. X _{TOC} = 10.13 % probably due to adsorption	[38]
Paracetamol 35 µmol/L	γ -Al ₂ O ₃	cat. 5 mg/L, pH 7, [O ₃] _{dose} = 3 mg/min, t _{test} = 1 h, SemiBatch reactor	O ₃ X _{TOC} = 18 % O ₃ + cat. X _{TOC} = 17.2 %	[38]
Oxalic acid TOC ₀ = 60 mg/L	γ -Al ₂ O ₃	cat. 50 g/L, V _{liq} = 40 mL, pH 3.3, [O ₃] _{gas} = 50 g/Nm ³ , t _{test} = 30 min, Batch reactor	Ads. X _{TOC} = 71.9 % O ₃ X _{TOC} = 26.5 % O ₃ + cat. X _{TOC} = 73.6 %	[23]
Oxalic acid TOC ₀ = 60 mg/L	γ -Al ₂ O ₃	cat. 50 g/L, V _{liq} = 40 mL, pH 5 (buffer orthophosphate), [O ₃] _{gas} = 50 g/Nm ³ , t _{test} = 30 min, Batch reactor	Ads. X _{TOC} = 8.8 % O ₃ X _{TOC} = 0.2 % O ₃ + cat. X _{TOC} = 19 %	[23]
Acetic acid TOC ₀ = 60 mg/L	γ -Al ₂ O ₃	cat. 50 g/L, V _{liq} = 40 mL, pH 3.3, [O ₃] _{gas} = 50 g/Nm ³ , t _{test} = 30 min, Batch reactor	Ads. X _{TOC} = 5.1 % O ₃ X _{TOC} = 4.2 % O ₃ + cat. X _{TOC} = 7.7 %	[23]
Acetic acid TOC ₀ = 60 mg/L	γ -Al ₂ O ₃	cat. 50 g/L, V _{liq} = 40 mL, pH 5 (buffer orthophosphate), [O ₃] _{gas} = 50 g/Nm ³ , t _{test} = 30 min, Batch reactor	Ads. X _{TOC} = 0 % O ₃ X _{TOC} = 2.2 % O ₃ + cat. X _{TOC} = 0 %	[23]
Salicylic acid TOC ₀ = 60 mg/L	γ -Al ₂ O ₃	cat. 50 g/L, V _{liq} = 40 mL, pH 3.3, [O ₃] _{gas} = 50 g/Nm ³ , t _{test} = 30 min, Batch reactor	Ads. X _{TOC} = 60.8 % O ₃ X _{TOC} = 38.6 % O ₃ + cat. X _{TOC} = 89.9 %	[23]
Salicylic acid TOC ₀ = 60 mg/L	γ -Al ₂ O ₃	cat. 50 g/L, V _{liq} = 40 mL, pH 5 (buffer orthophosphate), [O ₃] _{gas} = 50 g/Nm ³ , t _{test} = 30 min, Batch reactor	Ads. X _{TOC} = 41.4 % O ₃ X _{TOC} = 44.9 % O ₃ + cat. X _{TOC} = 83.5 %	[23]
Succinic acid TOC ₀ = 60 mg/L	γ -Al ₂ O ₃	cat. 50 g/L, V _{liq} = 40 mL, pH 3.3, [O ₃] _{gas} = 50 g/Nm ³ , t _{test} = 30 min, Batch reactor	Ads. X _{TOC} = 24.2 % O ₃ X _{TOC} = 5.8 % O ₃ + cat. X _{TOC} = 87.5 %	[23]
Succinic acid TOC ₀ = 60 mg/L	γ -Al ₂ O ₃	cat. 50 g/L, V _{liq} = 40 mL, pH 5 (buffer orthophosphate), [O ₃] _{gas} = 50 g/Nm ³ , t _{test} = 30 min, Batch reactor	Ads. X _{TOC} = 0.4 % O ₃ X _{TOC} = 0 % O ₃ + cat. X _{TOC} = 69.2 %	[23]
Succinic acid TOC ₀ = 60 mg/L	χ - and η -Al ₂ O ₃	cat. 50 g/L, V _{liq} = 40 mL, pH 5 (buffer orthophosphate), [O ₃] _{gas} = 50 g/Nm ³ , t _{test} = 30 min, Batch reactor	Ads. X _{TOC} = 18.8 % O ₃ + cat. X _{TOC} = 35 %	[23]
Succinic acid TOC ₀ = 60 mg/L	χ - and η -Al ₂ O ₃	cat. 20 g/L, V _{liq} = 5.2 L, pH 7, Q _{gas} = 100 L/h, [O ₃] _{gas} = 50 g/Nm ³ , t _{test} = 1 h, Slurry SemiBatch reactor	O ₃ X _{TOC} = 23 % O ₃ + cat. X _{TOC} = 90 %	[23]
Diclofenac 30 mg/L	γ -Al ₂ O ₃	cat. 5 g, V _{liq} = 250 mL, pH 7 or 5, Q _{gas} = 25 L/h, [O ₃] _{gas} = 20 mg/L, t _{test} = 2 h, Batch reactor	O ₃ X _{TOC} = 40 %, pH 7: O ₃ + cat. X _{TOC} = 65 % pH 5: O ₃ + cat. X _{TOC} = 40 % Adsorption of carboxylates was confirmed	[39]
2-methylisborneol (MIB) 22 µg/L	γ -Al ₂ O ₃	cat. 500 mg/L, V _{liq} = 1 L, 20°C, pH 6.6, [O ₃] _{liq} = 0.5 mg/L, t _{test} = 20 min, Batch reactor	Ads. X _{MIB} = 2.5 % O ₃ X _{MIB} = 40 % O ₃ + cat. X _{MIB} = 87 %	[40]

4-chloro-7-nitrobenzo-2-oxa-1,3-dizole (NBD-Cl) 20 mg/L	γ -Al ₂ O ₃	cat. 2 g, V _{liq} = 0.49 L, 25°C, pH 8.8, [O ₃] _{dose} = 0.6 mg/min, t _{test} = 30 min, SemiBatch reactor	Ads. X _{NBD-Cl} = 4-5 % O ₃ X _{NBD-Cl} = 40 % O ₃ + cat. X _{NBD-Cl} = 72 %	[41]
2-chlorophenol (CP) 100 mg/L	γ -Al ₂ O ₃	cat. 2 g/L, pH 7, [O ₃] _{dose} = 18 mg/min, t _{test} = 90 min, SemiBatch reactor	Ads. X _{CP} = 1.1-2.2 % O ₃ X _{TOC} = 21 % O ₃ + cat. X _{TOC} = 43 %	[42]
2, 4, 6-trichloroanisole (TCA) 25 µg/L	γ -Al ₂ O ₃	cat. 200 mg/L, V _{liq} = 1 L, 20 °C, pH 5.8, [O ₃] _{0liq} = 0.5 mg/L, t _{test} = 10 min, Batch reactor	Ads. X _{TCA} = 10 % O ₃ X _{TCA} = 40 % O ₃ + cat. X _{TCA} = 62 %	[43]
Ibuprofen 10 mg/L	γ -Al ₂ O ₃	cat. 1.5 g/L, V _{liq} = 1 L, 20°C, pH ₀ 7, Q _{gas} = 12 L/h, [O ₃] _{gas} = 30 mg/L, t _{test} = 40 min, SemiBatch reactor	O ₃ X _{TOC} = 20 % O ₃ + cat. X _{TOC} = 54 %	[44]
Ibuprofen (IBU) 10 mg/L	β -FeOOH/ γ -Al ₂ O ₃	cat. 1.5 g/L, V _{liq} = 1 L, 20°C, pH ₀ 7, Q _{gas} = 12 L/h, [O ₃] _{gas} = 30 mg/L, t _{test} = 40 min, SemiBatch reactor	Ads. X _{IBU} < 5 % O ₃ X _{TOC} = 20 % O ₃ + cat. X _{TOC} = 90 %	[44]
m-cresol 9.52 mol/L	γ -Al ₂ O ₃	cat. 10 g/L, V _{liq} = 25 mL, 20 °C, Q _{gas} = 0.5 L/min, [O ₃] _{gas} = 0.123 mg/L, t _{test} = 24 h, SemiBatch reactor	O ₃ X _{m-cresol} = 22.5 % O ₃ + cat. X _{m-cresol} = 47 %	[45]
Sulfamethoxazole TOC ₀ = 15 mg/L	Al ₂ O ₃	20°C, pH 7, Q _{gas} = 24 L/h, [O ₃] _{gas} = 20 mg/L, t _{test} = 2 h, Slurry SemiBatch reactor	O ₃ X _{TOC} = 28 % O ₃ + cat. X _{TOC} = 39 %	[22]
Textile wastewater COD ₀ = 180 mg/L	Al ₂ O ₃	cat. 300 g, pH 4, Q _{liq} = 250 L/h, Q _{gas} = 340 L/h, expanded bed height = 17 cm, [O ₃] _{gas} = 0.9 mmol/L, Continuous fluidized bed reactor	O ₃ X _{COD} = 16.49 % O ₃ + cat. X _{COD} = 25.83 %	[46]
Petroleum refinery wastewater COD ₀ = 101.3 mg/L	γ -Al ₂ O ₃	cat. 0,5 g, V _{liq} = 100 mL, 30°C, pH 8.15, O ₃ 5 mg/min, t _{test} = 40 min, Slurry SemiBatch reactor	Ads. X _{COD} = 8.5 % O ₃ X _{COD} = 34.3 % O ₃ + cat. X _{COD} = 45.9 %	[47]
Fluoxetine 30 mg/L	γ -Al ₂ O ₃	cat. 1 g/L, V _{liq} = 200 mL, 25°C, pH 7, [O ₃] _{gas} = 30 mg/L, t _{test} = 17 min, Slurry SemiBatch reactor	O ₃ X _{fluox} = 80 % O ₃ + cat. X _{fluox} = 86 %	[48]
Naphtenic acids 100 mg/L	γ -Al ₂ O ₃	cat. 1 g/L, 25°C, pH 8.5, Q _{gas} = 1 L/min, t _{test} = 50 min, Slurry Batch reactor	Ads. X _{naph} = 8 % O ₃ X _{naph} = 85 % O ₃ + cat. X _{naph} = 88 %	[49]
Humic acids 50 mg/L	α -Al ₂ O ₃	cat. 0,5 g/L, 25°C, pH 5.5, O ₃ 0.063 m ³ /h, t _{test} = 1 h, Slurry Batch reactor	Ads. X _{humic} = 90 % O ₃ X _{humic} = 81 % O ₃ + cat. X _{humic} = 100 %	[50]
Landfill leachate COD ₀ = 1317.5 mg/L	γ -Al ₂ O ₃	cat. 50 g/L, V _{liq} = 300 mL, 30°C, pH ₀ 7.3, O ₃ 22 mg/min, t _{test} = 30 min, Slurry SemiBatch reactor	Ads. X _{COD} = 27 % O ₃ X _{COD} = 48 % O ₃ + cat. X _{COD} = 70 %	[51]

Table 2. Literature reports on different solids in the ozonation of SMX.

SMX Concentration	Solid material	Operating conditions	Removal results	Ref.
TOC ₀ = 15 mg/L	Al ₂ O ₃	20 °C, pH 7, Q _{gas} = 24 L/h, [O ₃] _{gas} = 25 mg/L, t _{test} = 2 h, Slurry SemiBatch reactor	Ads. X _{SMX} = 7 % O ₃ X _{TOC} = 28 % O ₃ + cat. X _{TOC} = 39 %	[22]
TOC ₀ = 15 mg/L	LaTi _{0.15} Cu _{0.05} O ₃	20 °C, pH 7, Q _{gas} = 24 L/h, [O ₃] _{gas} = 25 mg/L, t _{test} = 2 h, Slurry SemiBatch reactor	Ads. X _{SMX} = 1 % O ₃ X _{TOC} = 28 % O ₃ + cat. X _{TOC} = 85 %	[22]
TOC ₀ = 15 mg/L	Activated carbon Derco 15-20	20 °C, pH 7, Q _{gas} = 24 L/h, [O ₃] _{gas} = 25 mg/L, t _{test} = 2 h, Slurry SemiBatch reactor	Ads. X _{SMX} = 100 % O ₃ X _{TOC} = 28 % O ₃ + cat. X _{TOC} = 92 % Organic matter resulting from preozonation times >10 min, hardly adsorbs onto activated carbon	[22]
50 mg/L	Activated carbon Norbit GAC 1240 pluc	cat. 100 mg, V _{liq} = 0.7 L, pH 4.8, Q _{gas} = 150 mL/min, [O ₃] _{gas} = 50 g/Nm ³ , t _{test} = 3 h, Slurry SemiBatch reactor	Ads. X _{TOC} = 65 % O ₃ X _{TOC} = 35 % O ₃ + cat. X _{TOC} = 45 %	[52]
50 mg/L	Commercial multi-walled carbon nanotubes (MWCN) Nanocyl3100	cat. 100 mg, V _{liq} = 0.7 L, pH 4.8, Q _{gas} = 150 mL/min, [O ₃] _{gas} = 50 g/Nm ³ , t _{test} = 3 h, Slurry SemiBatch reactor	Ads. X _{TOC} = 30 % O ₃ X _{TOC} = 35 % O ₃ + cat. X _{TOC} = 35 %	[52]
50 mg/L	CeO ₂ AC	cat. 100 mg, V _{liq} = 0.7 L, pH 4.8, Q _{gas} = 150 mL/min, [O ₃] _{gas} = 50 g/Nm ³ , t _{test} = 3 h, Slurry SemiBatch reactor	Ads. X _{SMX} = 58 %, O ₃ X _{TOC} = 34 %, O ₃ + cat. X _{TOC} = 73 %	[53]
50 mg/L	CeO ₂ /MWCNT	cat. 100 mg, V _{liq} = 0.7 L, pH 4.8, Q _{gas} = 150 mL/min, [O ₃] _{gas} = 50 g/Nm ³ , t _{test} = 3 h, Slurry SemiBatch reactor	Ads. X _{SMX} = 33 % O ₃ X _{TOC} = 34 % O ₃ + cat. X _{TOC} = 56 %	[53]
50 mg/L	CeO ₂	cat. 100 mg, V _{liq} = 0.7 L, pH 4.8, Q _{gas} = 150 mL/min, [O ₃] _{gas} = 50 g/Nm ³ , t _{test} = 3 h, Slurry SemiBatch reactor	Ads. X _{SMX} = 0 % O ₃ X _{TOC} = 34 % O ₃ + cat. X _{TOC} = 61 %	[53]
TOC ₀ = 40 mg/L	Commercial activated carbon (PAC)	cat. 2 g/L, 26 °C, pH 5, Q _{gas} = 1 L/min, [O ₃] _{gas} = 48 mg/L, t _{test} = 20 min, Slurry SemiBatch reactor	O ₃ X _{TOC} = 37 % O ₃ + cat. X _{TOC} = 78 %	[3]
TOC ₀ = 40 mg/L	FeO ₃ /CeO ₂ loaded activated carbon (MOPAC)	cat. 2 g/L, 26 °C, pH 5, Q _{gas} = 1 L/min, [O ₃] _{gas} = 48 mg/L, t _{test} = 20 min, Slurry SemiBatch reactor	O ₃ X _{TOC} = 37 % O ₃ + cat. X _{TOC} = 86 %	[3]
Intermediates of 10 min ozonation of 0.0001 mol/L SMX	Activated carbon Darco 12-20 (PAC)	cat. 1 g/L, 20 °C, pH 7, Q _{gas} = 25 L/h, [O ₃] _{gas} = 20 mg/L, t _{test} = 40 min, Slurry SemiBatch reactor	Ads. X _{TOC} = 6 % O ₃ X _{TOC} = 17 % O ₃ + cat. X _{TOC} = 32 % (10 min)	[3]
50 mg/L	Treated Commercial multi-walled carbon nanotubes MWCN-HNO ₃ -N ₂ -900	cat. 100 mg, V _{liq} = 0.7 L, pH 4.8, Q _{gas} = 150 mL/min, [O ₃] _{gas} = 50 g/Nm ³ , t _{test} = 3 h, Slurry SemiBatch reactor	Ads. X _{SMX} = 55 % O ₃ X _{TOC} = 35 % O ₃ + cat. X _{TOC} = 45 %	[54]
50 mg/L	Treated Commercial multi-walled carbon nanotubes MWCN-O ₂	cat. 100 mg, V _{liq} = 0.7 L, pH 4.8, Q _{gas} = 150 mL/min, [O ₃] _{gas} = 50 g/Nm ³ , t _{test} = 3 h, Slurry SemiBatch reactor	Ads. X _{SMX} = 38 % O ₃ X _{TOC} = 35 % O ₃ + cat. X _{TOC} = 41 %	[54]
0.0003 mol/L	Fe ²⁺ -Montmorillonite	cat. 1 g/L, pH ₀ 2.88, [O ₃] _{dose} = 5 mg/min, t _{test} = 20 min, Slurry SemiBatch reactor	O ₃ + cat. X _{COD} = 97 %	[55]
50 mg/L	Magnetic Fe ₃ O ₄ nanoparticles	cat. 1 g/L, V _{liq} = 0.2 L, 25 °C, [O ₃] _{dose} = 2 g/h, t _{test} = 5 min, Slurry SemiBatch reactor	O ₃ X _{SMX} = 85 % O ₃ + cat. X _{SMX} = 97 %	[56]

50 mg/L	Heteroatom doped graphene oxide PGO	cat. 1 g/L, 25 °C, pH 9, $[O_3]_{dose} = 2$ g/h, $t_{test} = 5$ min, Slurry SemiBatch reactor	$O_3 X_{SMX} = 62\%$ $O_3 + cat. X_{SMX} = 99\%$	[57]
10 mg/L	γ -Ti-Al ₂ O ₃	cat. 1.5 g, $V_{liq} = 1$ L, pH 7, $Q_{gas} = 200$ mL/min, $[O_3]_{gas} = 30$ mg/Nm ³ , $t_{test} = 1$ h, Slurry SemiBatch reactor	Ads. $X_{SMX} = 8\%$ $O_3 X_{TOC} = 26\%$ $O_3 + cat. X_{TOC} = 92\%$	[58]
25.3 mg/L	Iron-manganese silicate oxide	cat. 0.5 g, $V_{liq} = 0.5$ L, pH ₀ 7, $Q_{gas} = 0.4$ L/min, $[O_3]_{gas} = 9.05$ mg/L, $t_{test} = 1$ h, Slurry SemiBatch reactor	Ads. $X_{SMX} = 1.8\%$ $O_3 X_{TOC} = 27\%$ $O_3 + cat. X_{TOC} = 79.8\%$ Adsorption of SMX intermediates at 30 min (cat. 0,1 g/L) = 17.9 %	[24]
30 mg/L SMX + 30 mg/L diclofenac	Fe-Mn-O	cat. 1 g/L, pH ₀ 5.5, $Q_{gas} = 2$ L/min, $[O_3]_{gas} = 10$ g/m ³ , $t_{test} = 2$ h, Slurry SemiBatch reactor	$O_3 X_{TOC} = 44\%$ $O_3 + cat. X_{TOC} = 63\%$	[59]

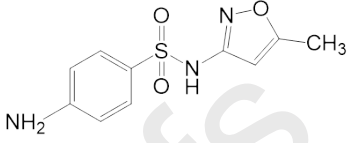
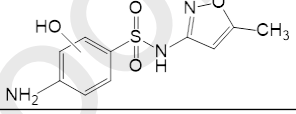
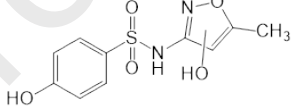
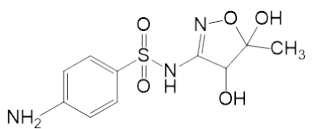
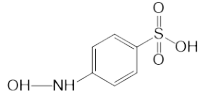
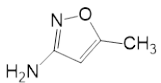
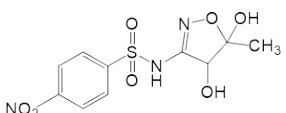
Table 3. Characterization of the municipal secondary effluent used in this work.

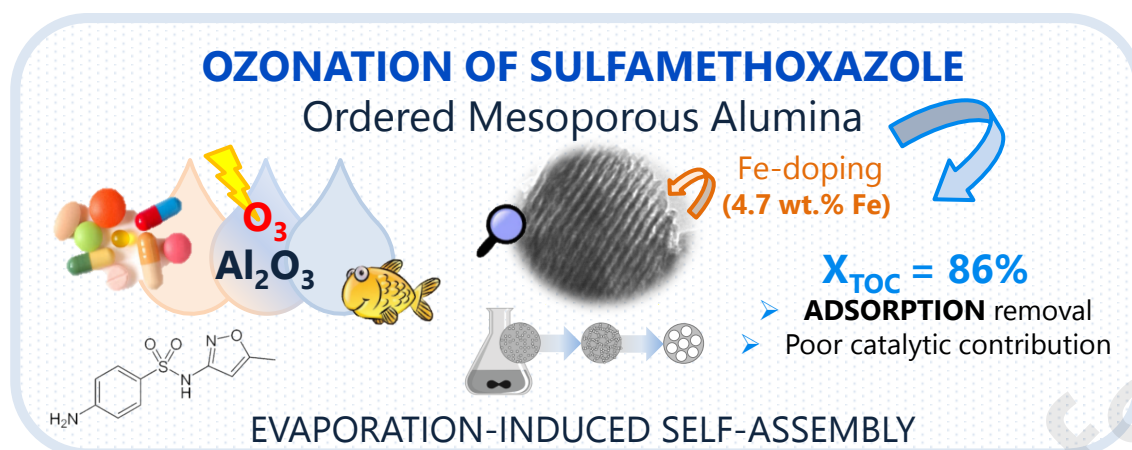
Parameter	Mean value
pH	7.85
TC, mg/L	38.5
TOC, mg/L	20.68
COD, mg O ₂ /L	79.5
Filtered COD, mg O ₂ /L	68.8
UVA ₂₅₄	0.156
Turbidity, NTU	0.9
Alkalinity, mg CaCO ₃ /L	346.2
Cl, mg/L	32.41
Na, mg/L	611.46
Ca, mg/L	99.34
Mg, mg/L	57.96
Total Solids, mg/L	2.36

Table 4. Summary of characterization outcomes.

Sample	S_{BET} (m^2/g)	V_{pore} (cm^3/g)	d_{pore} (nm)	PZC	Acid sites (mmol/g)	Pyridine desorption temperature ($^{\circ}\text{C}$)
MA	263	0.79	10.2	7.7	0.130	235
MA-5Fe	211	0.55	9.67	7.5	0.200	235
CA	200	0.50	7.15	7.6	0.097	227

Table 5. Accurate mass measurements found by LC-ESI(+)-TOF-MS spectra of protonated SMX and its degradation products.

Compound	Retention time (min)	Chemical formula	Experimental mass (m/z)	Probable reaction involved	O ₃ + MA-5Fe	O ₃	Structural formula	Reference
					Reaction time (min)	Reaction time (min)		
SMX	4.226	C ₁₀ H ₁₂ N ₃ O ₃ S	254.0596	None	1, 2, 4, 6, 8, 10, 15	1, 2, 4, 6, 8, 10, 15		[65–67]
		C ₆ H ₆ NO ₂ S	156.0121					
		C ₆ H ₆ NO	108.0442					
		C ₄ H ₇ N ₂ O	99.0562					
		C ₆ H ₇ N	93.0566					
		C ₆ H ₆ N	92.0498					
		C ₁₀ H ₁₁ N ₃ NaO ₃ S	276.0412					
C ₂₀ H ₂₂ N ₆ NaO ₆ S ₂	529.0933							
C1	3.852	C ₁₀ H ₁₂ N ₃ O ₄ S	270.0545	Benzene ring hydroxylation	1, 2, 4, 6, 8, 10	1, 2, 4, 6, 8		[66,67]
		C ₁₀ H ₁₁ N ₃ NaO ₄ S	292.0432					
		C ₄ H ₇ N ₂ O	99.057					
C2	3.510	C ₁₀ H ₁₁ N ₂ O ₅ S	271.0374	Isoxazole ring hydroxylation and amino group substitution	1, 2, 4, 6, 8, 10, 15	1, 2, 4, 6, 8, 10, 15		[65]
		C ₁₀ H ₁₀ N ₂ NaO ₅ S	293.0219					
C3	2.747	C ₁₀ H ₁₄ N ₃ O ₅ S	288.0641	Isoxazole ring dihydroxylation	2, 4, 6	1, 2, 4		[64,64–66]
		C ₁₀ H ₁₂ N ₃ O ₅ S	286.0484					
		C ₁₀ H ₁₀ N ₃ O ₅ S	284.0346					
		C ₁₀ H ₁₂ N ₃ O ₄ S	270.0543					
C4	2.291	C ₆ H ₈ NO ₄ S	190.0167	Aminophenylsulfone scission and amino group hydroxylation	2, 4, 6	ND		[67]
C5	3.114	C ₄ H ₇ N ₂ O	99.0559	Isoxazole ring scission	4, 6, 8, 10, 15	4, 6, 8, 10, 15, 30		[47,64–67]
		C ₃ H ₆ NO	72.0449					
C6	2.824	C ₁₀ H ₁₂ N ₃ O ₇ S	318.0398	Nitration of the amine group	ND	8, 10, 15		<i>This work</i>
		C ₁₀ H ₁₂ N ₃ O ₆ S	302.0449					
		C ₁₀ H ₁₄ N ₃ O ₅ S	288.0643					
		C ₁₀ H ₁₂ N ₃ O ₄ S	270.0547					



Highlights

- Ordered mesoporous alumina was synthesized by evaporation-induced self-assembly
- SMX was removed by direct O₃ attack, but its by-products were refractory towards O₃
- Alumina was able to decompose O₃ but displayed low catalytic effect in TOC removal
- Fe-Al₂O₃ achieved a remarkable TOC removal of 86% by chemisorption of carboxylates
- TOC removal occurred via ligand exchange mechanism and electrostatic interaction